NASA Contractor Report 170404

Variable Acuity Remote Viewing System Flight Demonstration

Ralph W. Fisher

Contract NAS4-2619
July 1983

National Aeronautics and
Space Administration

NASA Contractor Report 170404

Variable Acuity Remote Viewing System Flight Demonstration

Ralph W. Fisher
McDonnell Douglas Corporation
McDonnell Aircraft Company, P.O. Box 516, Saint Louis, Missouri 63166

Prepared for
Ames Research Center
Dryden Flight Research Facility
Edwards, California
under Contract NAS4-2619

1983

National Aeronautics and
Space Administration
Ames Research Center
Dryden Flight Research Facility
Edwards, California 93523

Use of trade names or names of manufacturers in this report does not constitute an official endorsement of such products or manufacturers, either expressed or implied, by the National Aeronautics and Space Administration.

TABLE OF CONTENTS

LIST OF ILLUSTRATIONS

LIST OF ILLUSTRATIONS (Continued)

LIST OF TABLES

This Page Intentionally Left Blank

1. INTRODUCTION AND SUMMARY

This report describes effort conducted under NASA (Dryden) contract NASA-2619, "Variable Acuity Remote Viewing System Flight Demonstration". The Variable Acuity Remote Viewing System (VARVS) has the capability to provide a wide field display (160°) at an RPV control station with resolution comparible to a conventional 20°-30° TV and requires no more transmission bandwidth. Since NASA (Dryden) research had generated indications that peripheral vision may play an important role in vehicle control they gave MCAIR this contract to modify the VARVS hardware, originally developed under contract to the Navy (ONR). The modifications were required to make the sensor compatible with their PA30 research aircraft and the display compatible with their existing RRPV cockpits. The final configurations of these equipment are shown in Figures 1 and 2. Details of the contracted effort are described in this report.

Due to unforeseen circumstances of a non technical nature the original objectives of the program were only partially met. However, some useful imagery (video tapes) were obtained during the program that are very effective in demonstrating the value of the Variable Acuity Display in vehicle control. Interested personnel are encouraged to view these tapes at NASA.

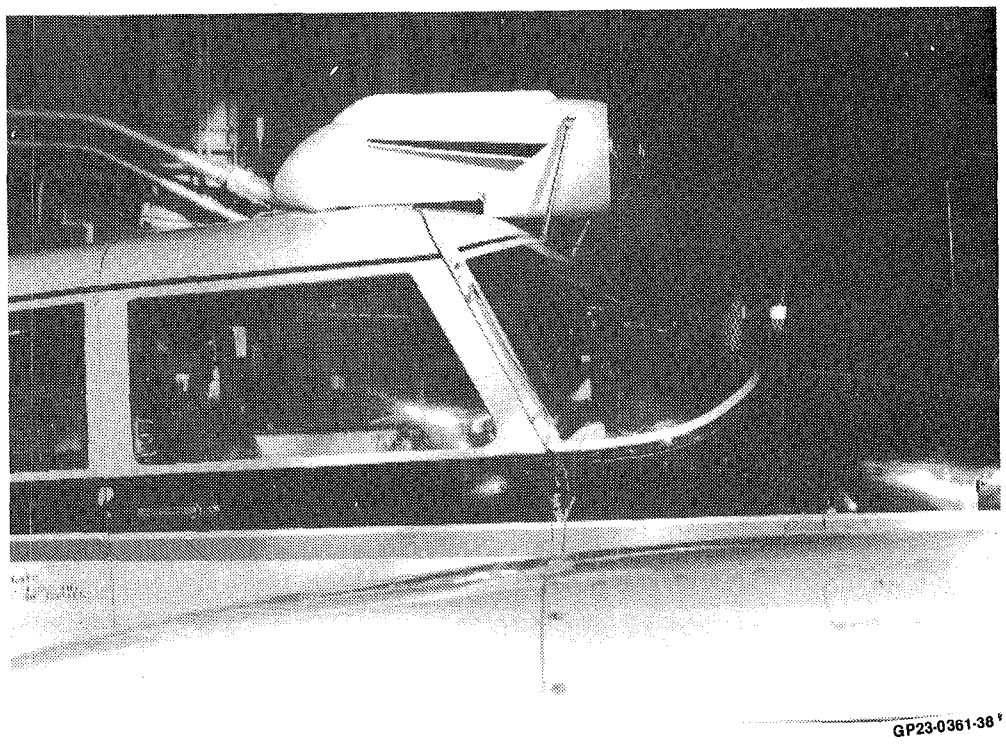

Figure 1. External Sensor Installation

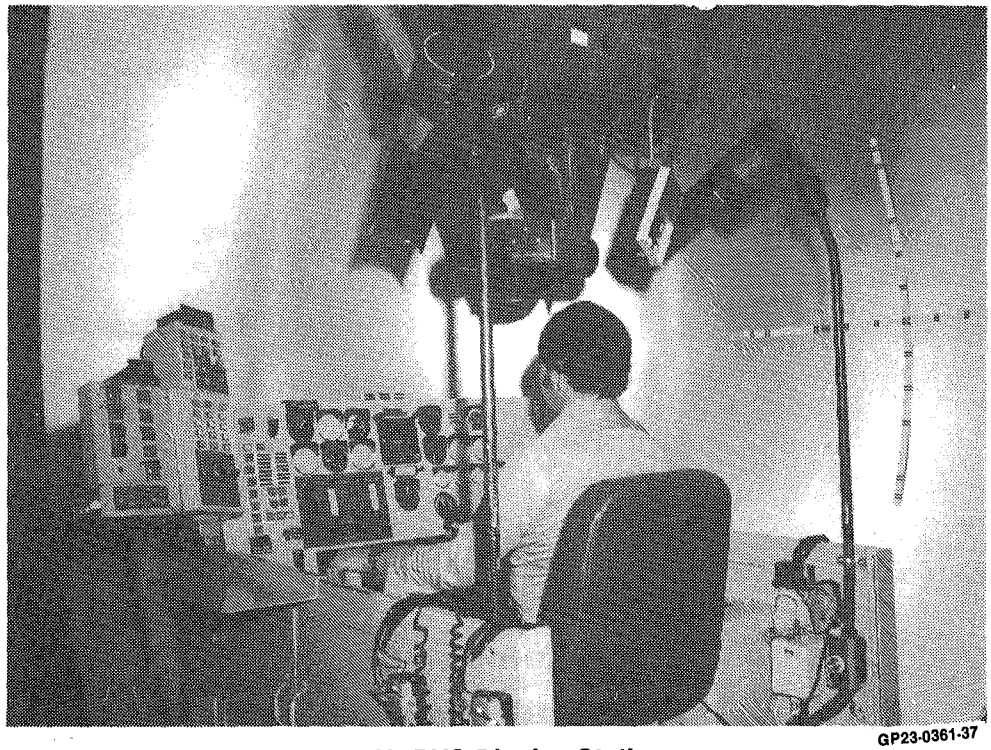

GP23-0361-37

Figure 2. VARVS Display Station

2. BACKGROUND

The Variable Acuity Remote Viewing System (VARVS) was conceived almost 10 years ago as a technique for circumventing the field of view/resolution/bandwidth tradeoffs that exist in remote viewing systems.

The system is based on the fact that only about 130,000 pixels are required to fully support human vision. This quantity is well within the capabilities of conventional TV systems. The problem was to develop a feasible technique that would take advantage of this fact.

The selected concept utilizes a non-linear optical system in both the sensing and display equipment. The non-linearity is achieved by a special lens which translates a uniform pixel array on its image plane into the object field as a variable angular array as described in Figure 3. This can be contrasted to the "Fish Eye" wide angle lens which projects into the object field with equal angular increments.

Another way of explaining the non-linearity of the special lens is that it will record the same angular detail the eye would see when viewing the same scene and compress this detail into a uniform matrix of equal sized picture elements on its image plane.

Mathematical integration of the human eye acuity function (Figure 3) shows that only 130,000 pixels exist within the total field of vision. The image can therefore be easily scanned by a conventional 525 line TV camera and transmitted to a remote location with conventional equipment. At the receiving end the image is reconstructed on a light valve projector and projected onto a spherical screen through an identical non-linear lens as shown on Figure 4.

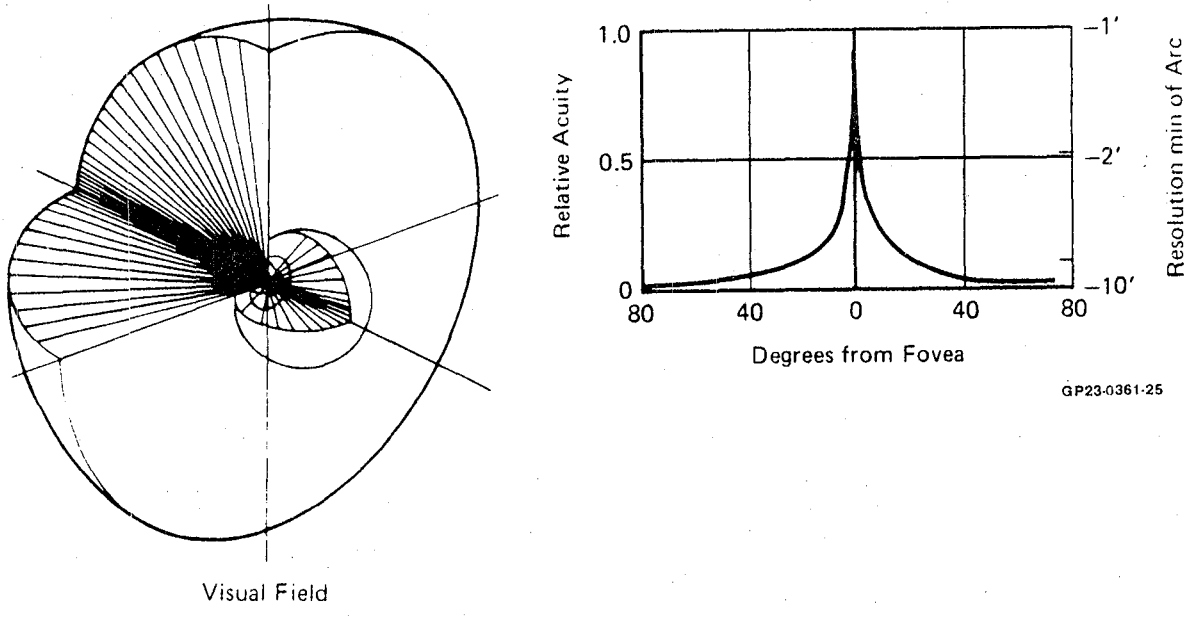

Figure 3. Human Eye Acuity

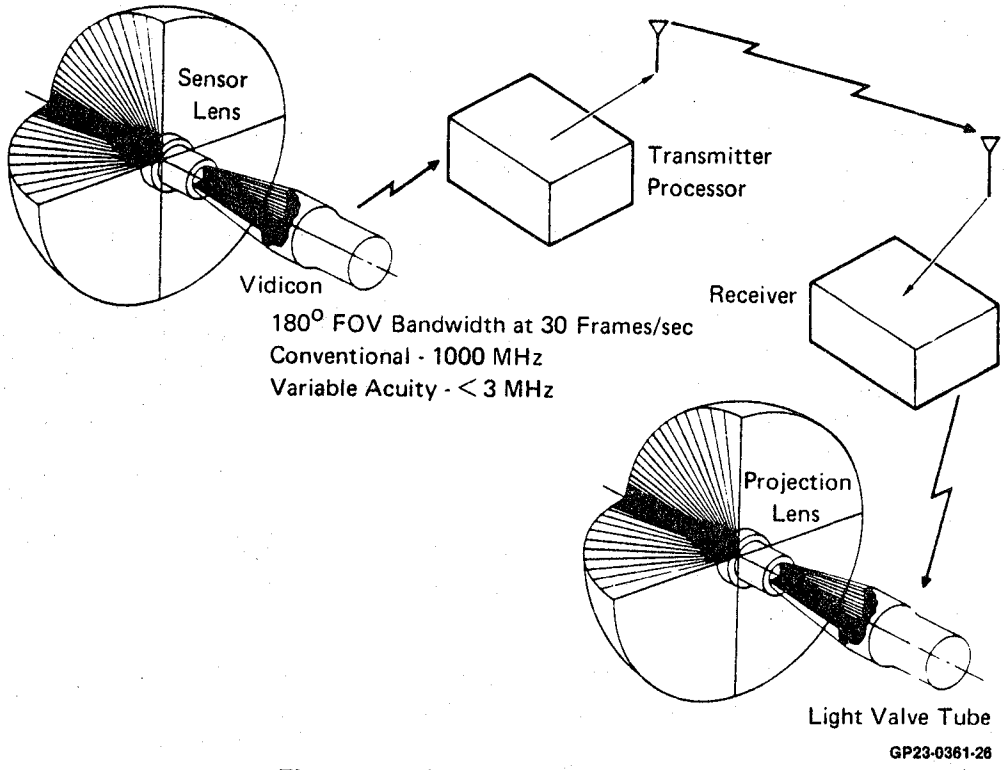

Figure 4. Electro-Optical Concept

The observer viewing the reconstructed picture sees things in correct geometric perspective and with apparent high acuity when his eye is aligned with the projector's optical axis. In the original VARVS concept an oculometer (eye position sensor) was postulated as a means to eliminate image to eye misalignment by repositioning the sensor through a narrow band control data link. In the present hardware, a simplified head-pointing system is used. The sensor gimbal positions are multiplexed with the video and transmitted to the display station where they are decoded and compared to head position. The difference is used to drive the projector gimbal system as shown in Figure 5. The result is high resolution along the head position axis. The display is vehicle referenced and appears just as it would be if the observer were located in the remote vehicle.

The key to feasibility of the concept is the non-linear lens. The lens was designed by MCAIR using a spline function approach and fabricated under contract to the Navy (ONR) using numerically controlled grinding machines (Reference 1). Details are shown in Figures 6 through 9. Two identical lenses were fabricated, one for the sensor and one for the projector. The focal length varies from 2 in. on axis to 0.05 in. at an 80° field angle. The image formed by the lens is about 0.72 in. in diameter.

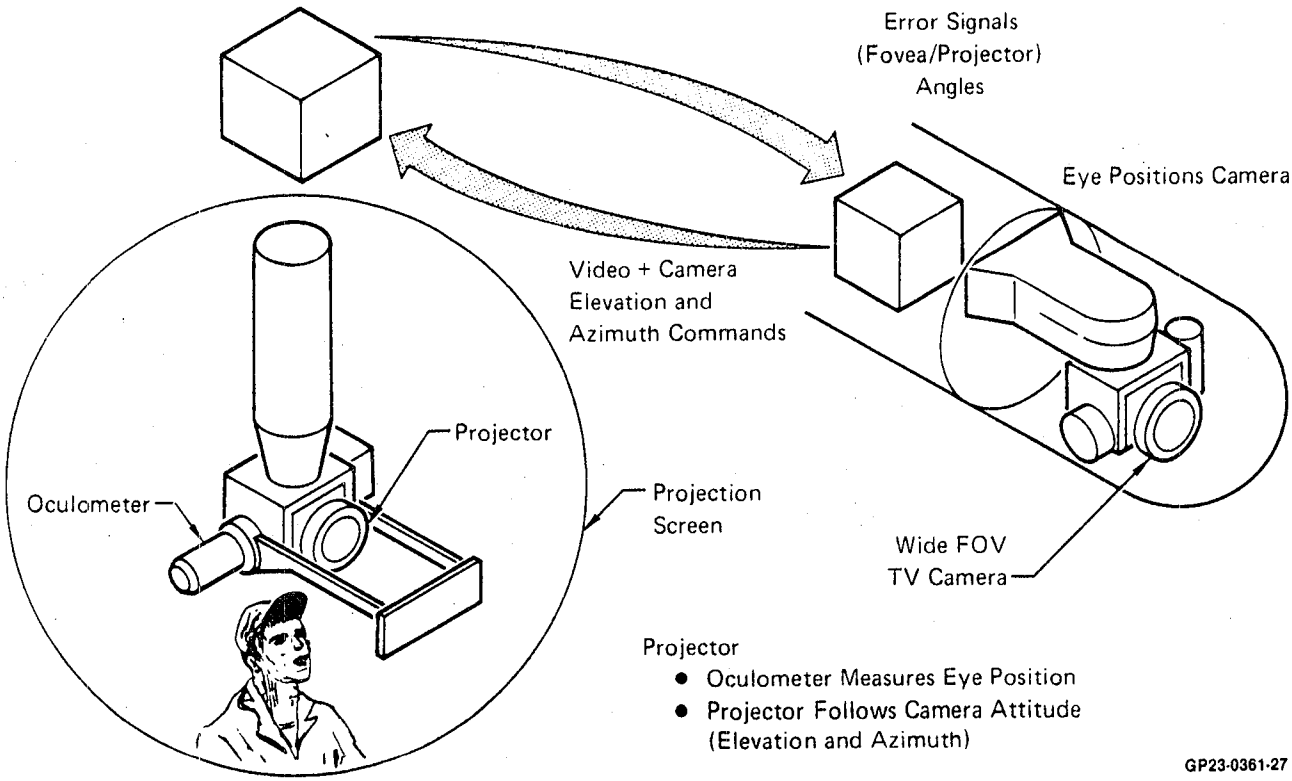

Figure 5. Control Concept

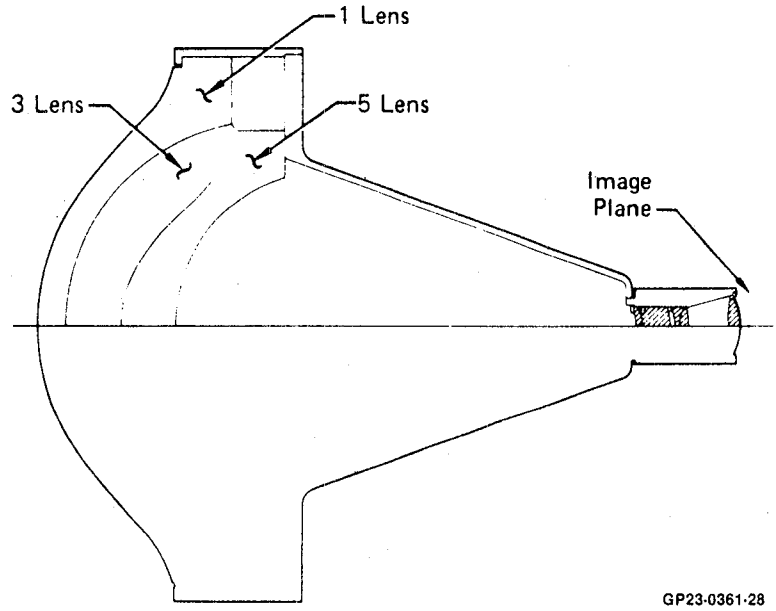

Figure 6. Lens Drawing

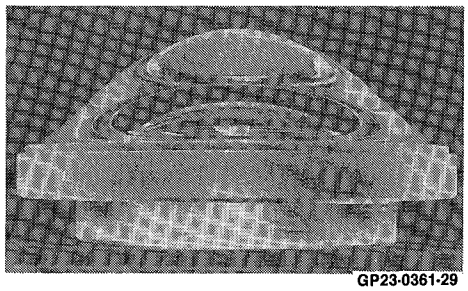

Figure 7. Front Lens Triplet

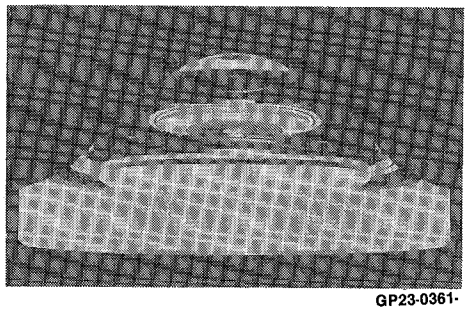

Figure 8. – 5 Spline

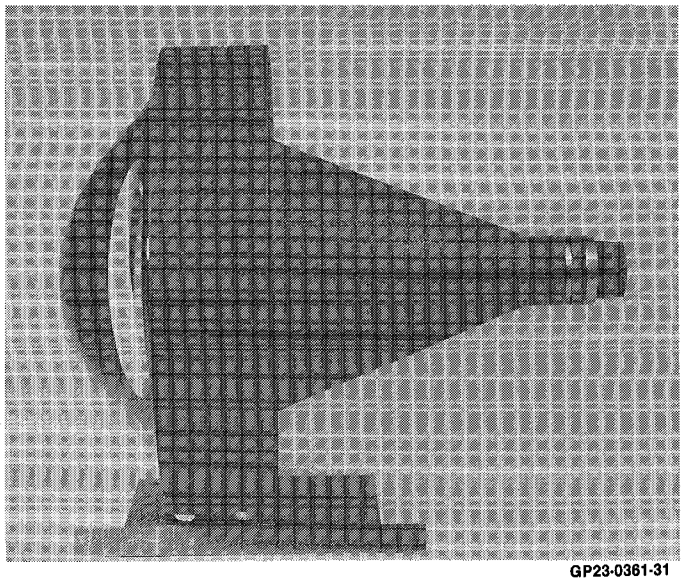

Figure 9. Nonlinear Lens

The extreme non-linearity of this lens can be demonstrated by comparing its image, Figure 10, to a fish eye image of the same scene, Figure 11. Note the high magnification that exists near the center of the image. A 525 line raster can extract the same angular detail from this image that would take a 10,000 line raster using the fish eye image.

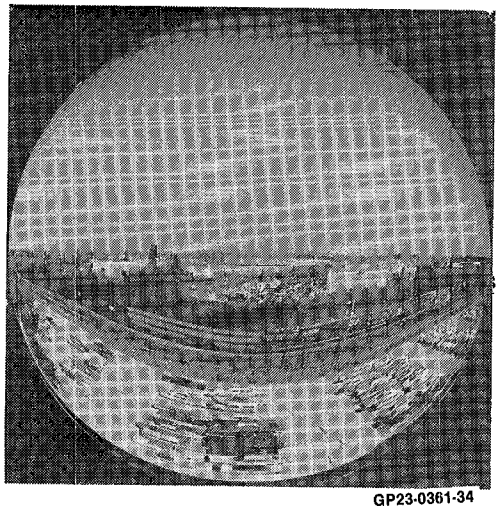

Figure 10. Nonlinear Lens Image

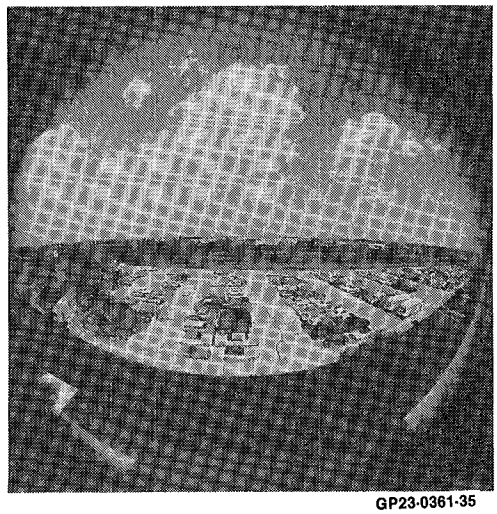

Figure 11. Fisheye Image

After lens feasibility was demonstrated, ONR funded fabrication of a brassboard demonstration system (Reference 2). A functional schematic of this effort is shown in Figure 12. The camera and projector hardware are shown in Figures 13 and 14.

Lab evaluation of this equipment was very successful. Head pointing control was proven to be very effective. The observer was found to adapt very quickly and had no difficulty keeping his foveal vision in the high acuity area.

Since NASA had evidence that a wide field display would be of value in RPV control, and had a manned research vehicle adapted for remote control plus the control stations, transmission data links, etc., they seemed a logical place to evaluate the VARVS system. The remainder of this report describes work required to adapt the VARVS hardware to the NASA facilities and the limited testing accomplished for the duration of the contract.

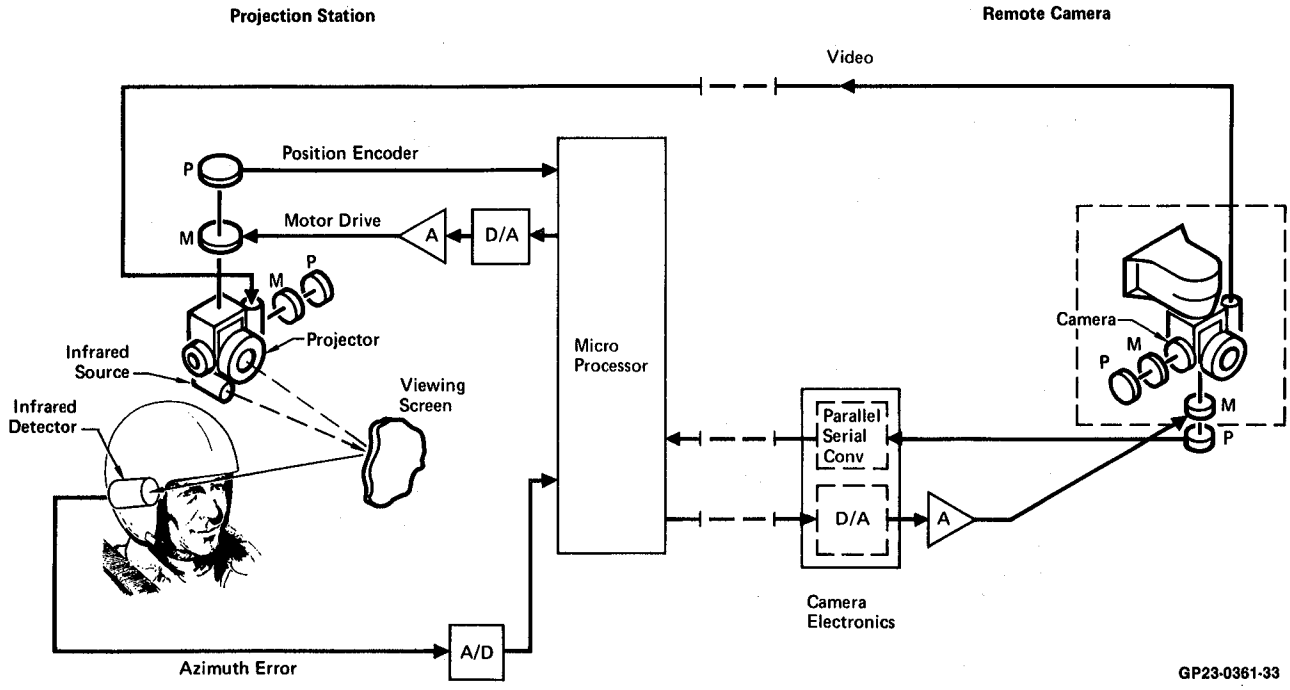

Figure 12. Control System Elements
Azimuth Axis Shown Only

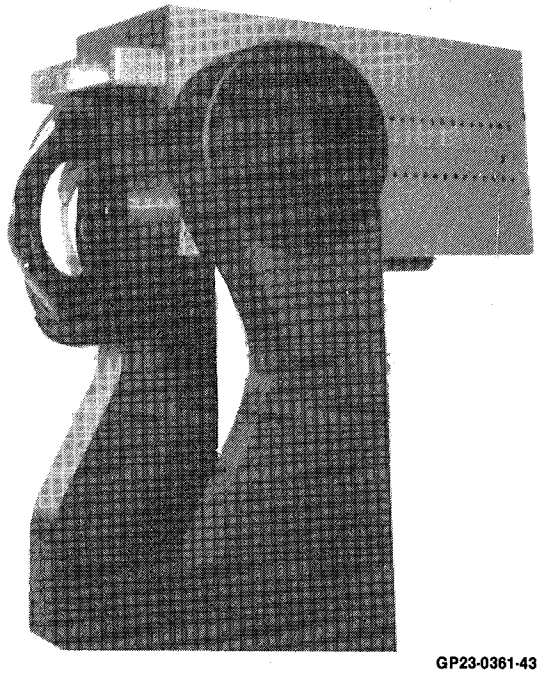

GP23-0361-43

Figure 13. Two-Axis Gimbaled Camera

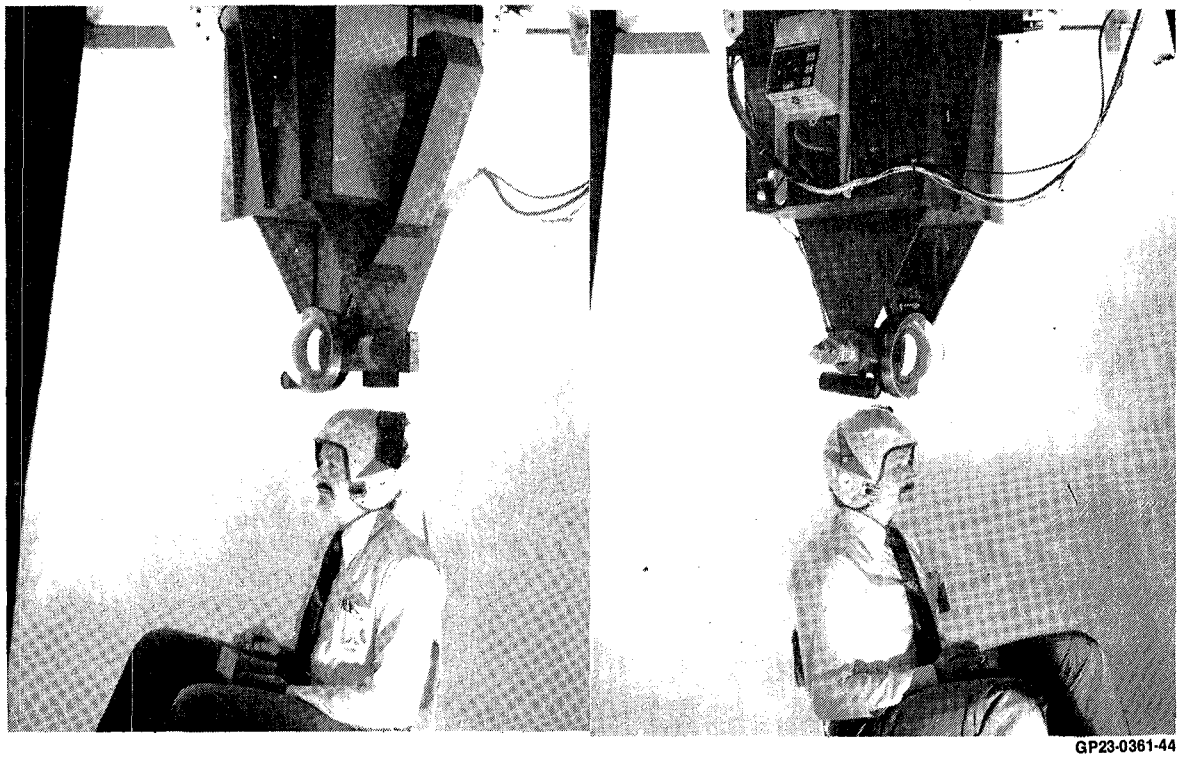

(a) Left Side Showing Detector Mounted on Helmet

(b) Right Side Showing Source on Projector Assembly

Figure 14. Projector

This Page Intentionally Left Blank

3. EQUIPMENT MODIFICATION/FABRICATION AT MCAIR

This work, performed prior to equipment shipment to EAFB, consisted of projector relay modification to improve brightness and resolution of the display, installation of a new TV camera on the sensor platform, inverting the platform to increase sensor visibility when mounted in the PA30 aircraft, and fabrication of a new display dome for the NASA installation. These efforts are described below:

3.1 PROJECTOR AND DISPLAY MODIFICATIONS

3.1.1 PROJECTOR RELAY MODIFICATIONS - The original VARVS brassboard hardware utilized a vertical raster scan. It was apparent during early tests that a conventional horizontal raster format would make more efficient use of the television raster and its associated transmission bandwidth. This is illustrated in Figure 15. Note the horizontal scan allows the lens image to occupy more of the raster. This means more detail will be extracted from the image at the sensor, and more of the available projector light output will be utilized in reprojecting the image.

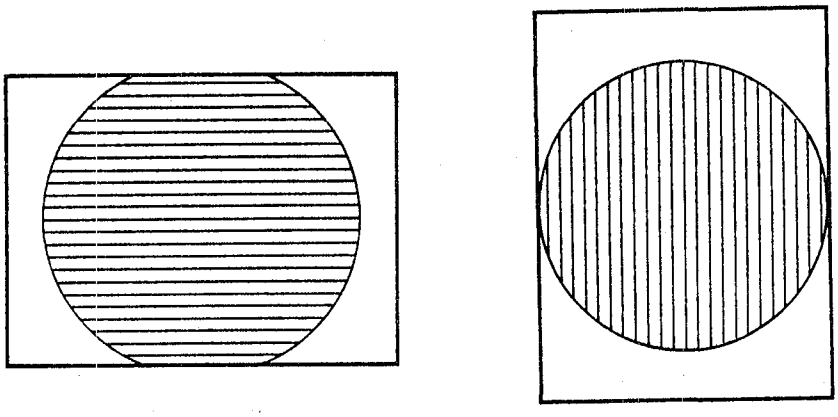

Figure 15. Raster Geometry

In the sensor the raster can be rotated by simply rotating the vidicon by 90°. In the projector this is not so simple. The light value requires a horizontal scan which is rotated 90° in relaying the image to the non-linear lens. Figure 16 shows primary elements of this relay. An image rotator is therefore required. Three possibilities existed for an image rotator. They are the dove prism, double dove prism and K mirror, as shown in Figure 17. The dove prism is clearly too long. The double dove originally appeared to be the best choice because it is shortest and would appear to have the smallest effect on the optical path. When one was tried experimentally serious loss in optical performance was observed. The problem was found to be associated with the Schlieren optical system of the light valve projector and the way the double dove recombines each half of the light bundle.

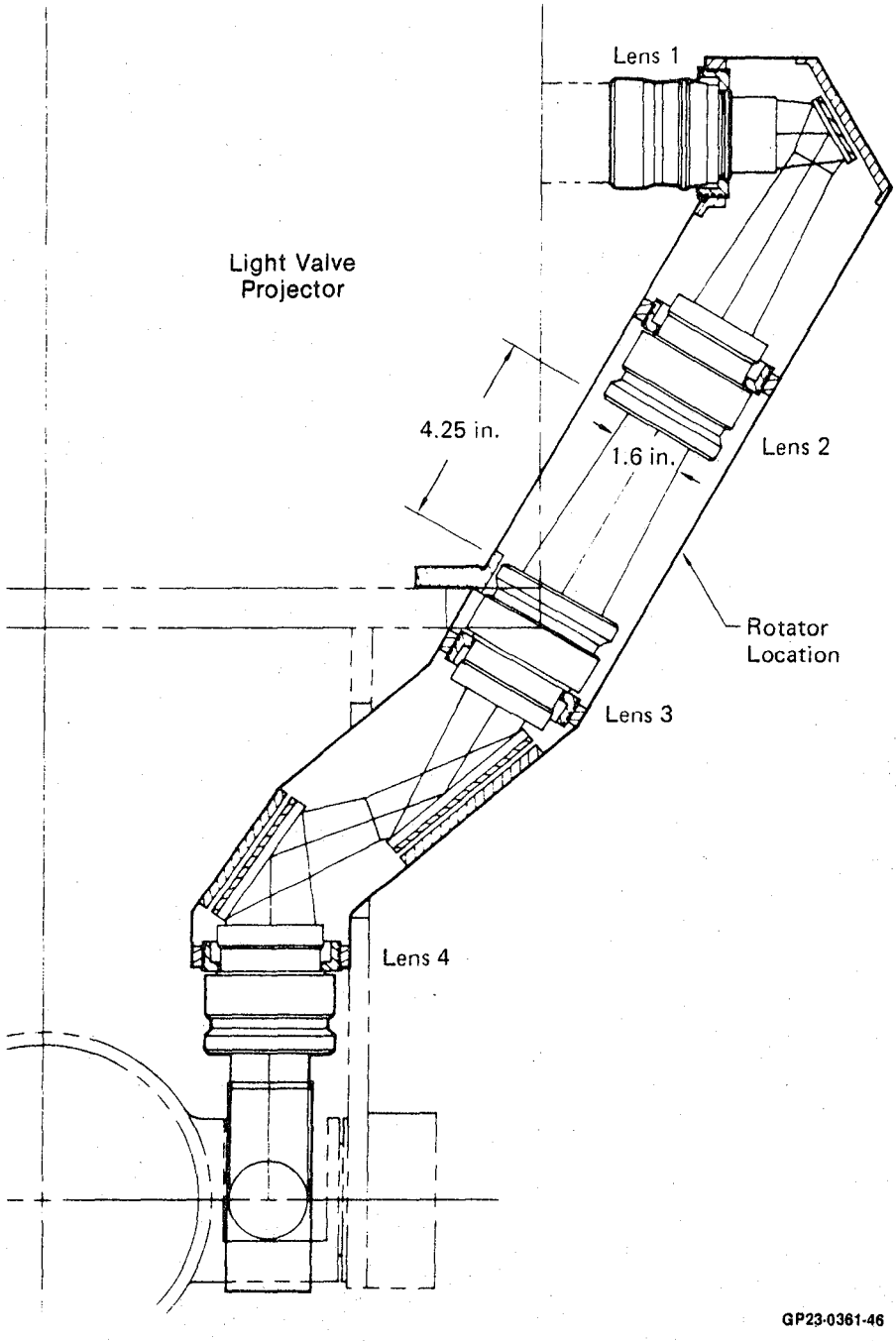

Figure 16. Original Relay Assembly

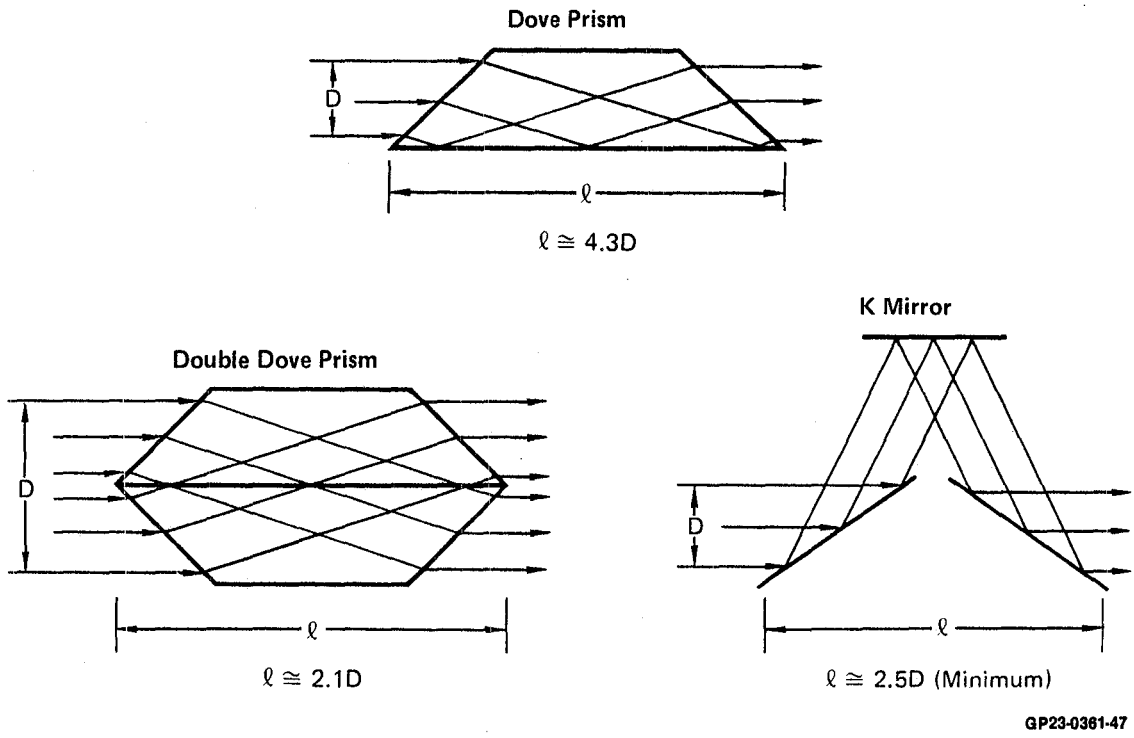

Figure 17. Image Rotators

Figure 18 shows how the double dove splits the input bundle and inverts each half before recombining. The effect on the non-linear lens is shown on the bottom of the figure. The result is a serious loss in brightness and resolution. Other problems found with the double dove were the high precision required in the optical surface angles, which leads to high fabrication costs.

The K mirror therefore evolves as the only possible choice for an image rotator. A K mirror was designed, fabricated, and installed in the optical relay. The design is shown in Figure 19.

The modified relay with the rotator installed is shown in Figure 20. A laser beam is directed through the relay to show the optical path more clearly. When the modified relay was installed in the projector system an extremely dim projection resulted. Measurements revealed that only 14% of the light valve output was reaching the non-linear lens. Removing the K mirror increased this to about 22%. Assuming 90% transmission for each lens, the transmission values with and without the K mirror indicate about 85% for mirror transmission, i.e.:

Without K Mirror	$T = 0.9^5 \times 0.85^6 = 0.22$
With K Mirror	$T = 0.9^5 \times 0.85^9 = 0.14$

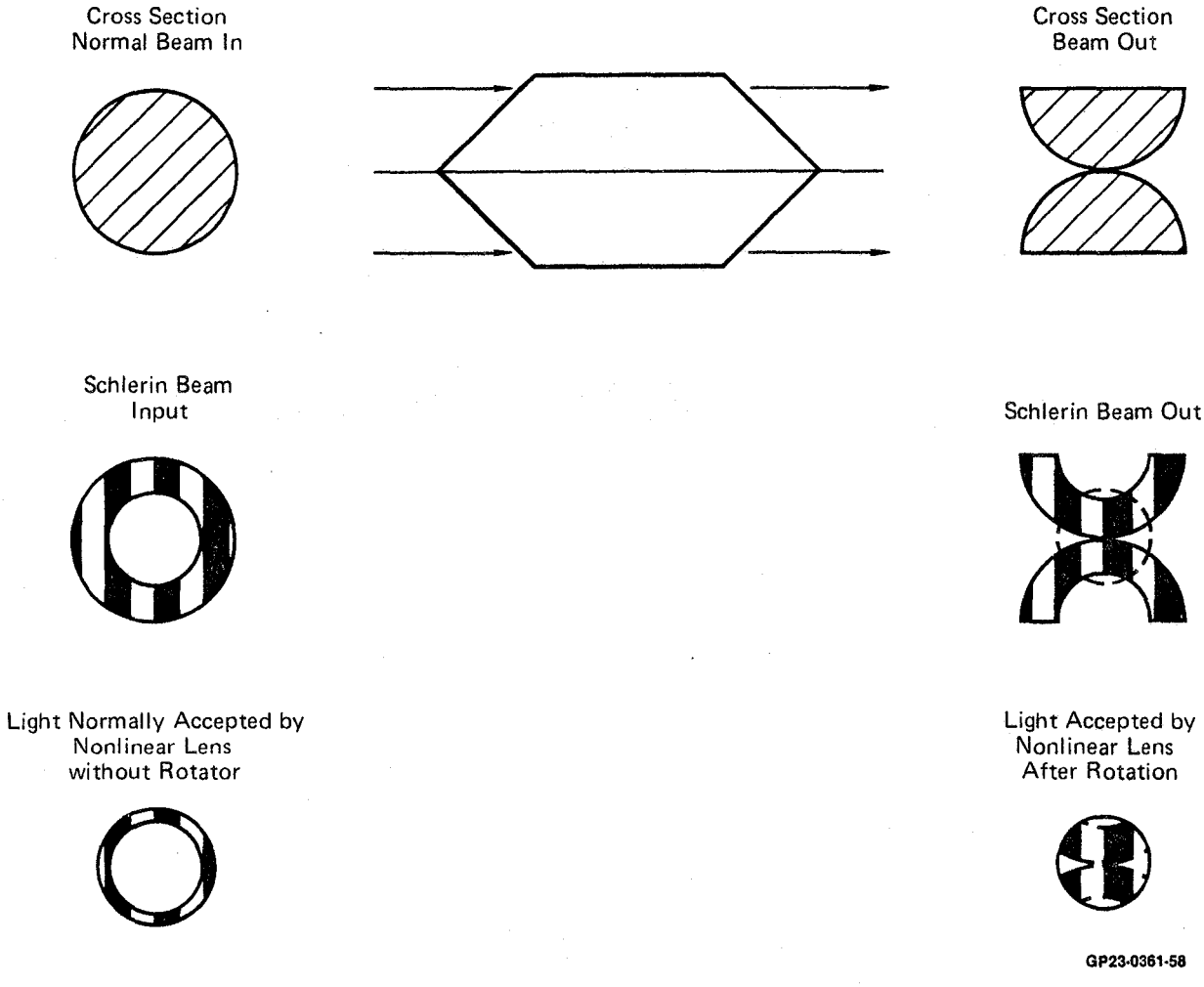

Figure 18. Double Dove Prism Problem

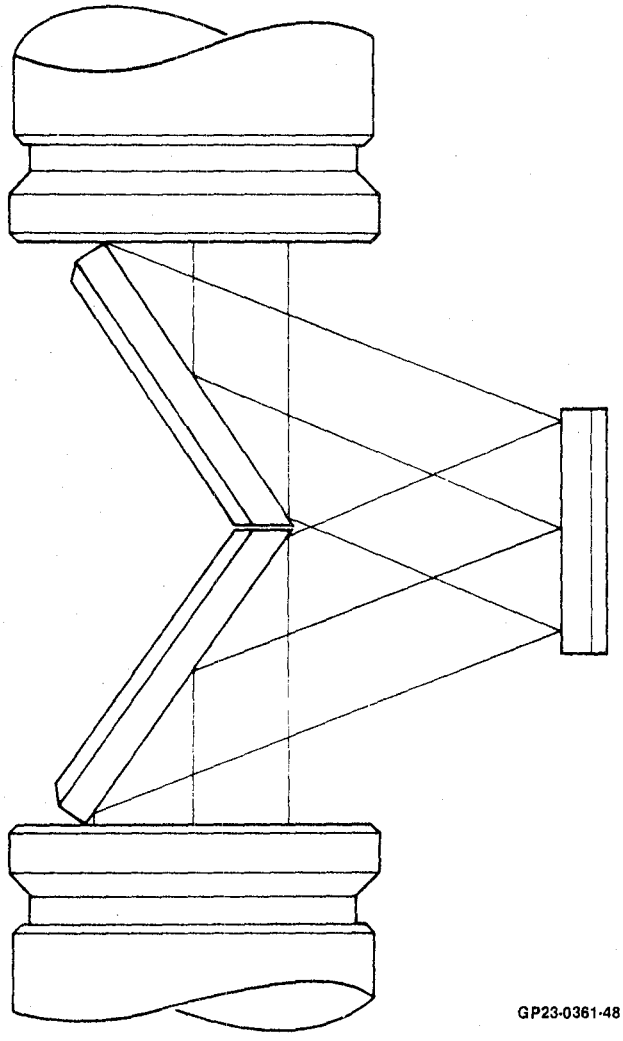

Figure 19. K Mirror Design

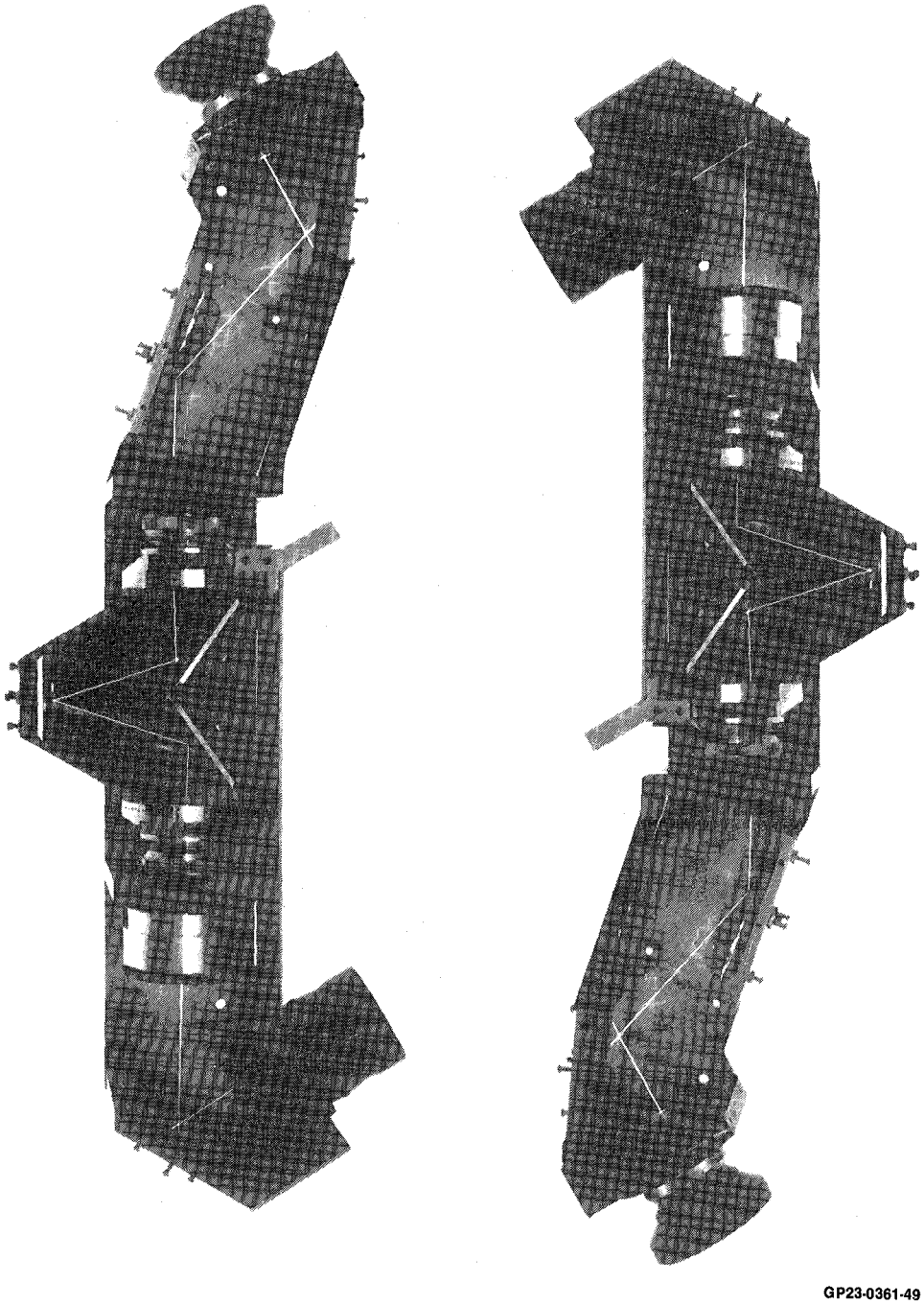

GP23-0361-49

Figure 20. Relay with Image Rotator

This difference was enough to change screen brightness from marginal to unacceptable. To improve the light level situation, all nine mirrors were removed from the projector and either refabricated or recoated. The new coating proved to have a tranmission of 0.93. The resulting relay transmission is

$$T = 0.9^5 \times 0.93^9 = 0.31$$

This produced very acceptable display brightness. However, a slightly yellow display color indicates high attenuation of shorter wavelengths. A more expensive broadband coating would correct this.

The longer optical path caused by the K mirror makes alignment more critical. Therefore, an improved alignment procedure was also developed. It is summarized in Table 1 and Figures 21 through 24.

TABLE 1. SUMMARY OF RELAY ALIGNMENT

1. Generate disk raster. (See Figure 21)
2. Check dark field alignment. (See Figure 22)
3. Collimate light valve.
4. Install the relay without the image rotator installed and adjust Mirror 1 so bundle centers on Lens 2 and Lens 3, (stop Lens 1 if necessary). (See Figure 23)
5. Check K Mirror alignment and reinstall in relay. (See Figure 24)
6. Autocollimate at Lens 4 - adjust Mirrors 2 and 3 for alignment.
   - Observe centering on Lens 4 diaphragm.
   - Observe angular alignment on Mirror 2 surface (stop Lens 2 to match normal to return spot size).
7. Adjust Lens 4 for collimation. (Remove Mirror 4, adjust screws to rotate bundle clear of structure).
8. Autocollimate on source side of Lens 5. Align Mirror 5 for return centered on Lens 4, (stop Lens 1 to reduce bundle size). Remove Return Mirror and observe horizontal centering through Lens 5. Translate Mirror 5 to correct. Adjust vertical alignment by simultaneous adjustment of Mirrors 4 and 5.
9. Align Mirror 6 for centered image at NLL. Translate to obtain flat image in horizontal direction.

GP23-0361-50

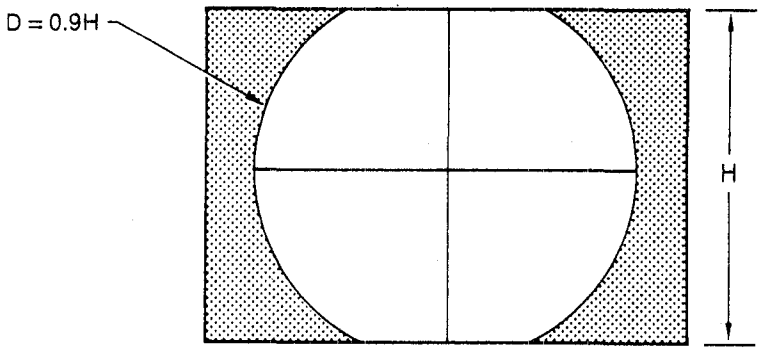

GP23-0361-51

Figure 21. Projector Raster Geometry

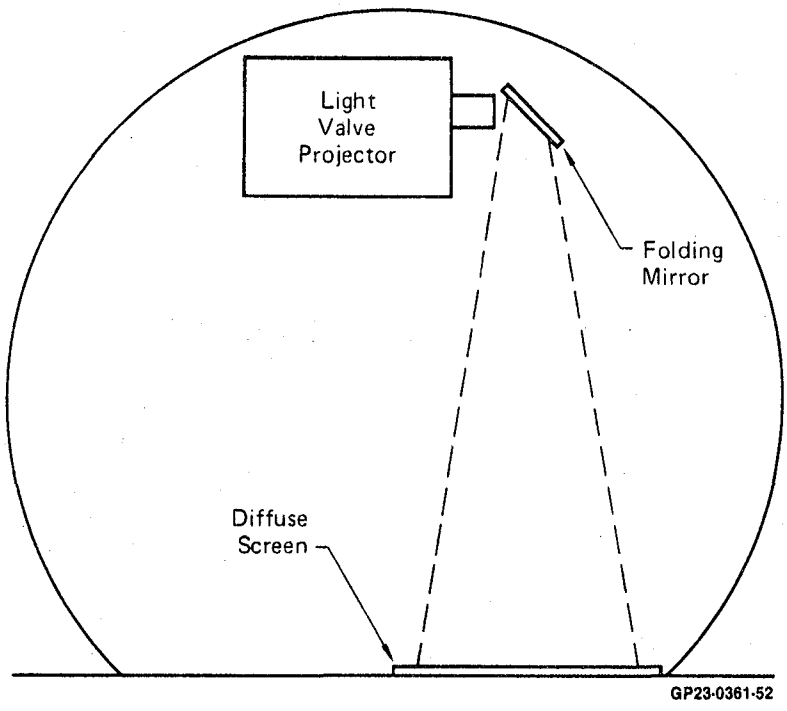

Figure 22. Setup for Light Valve Alignment

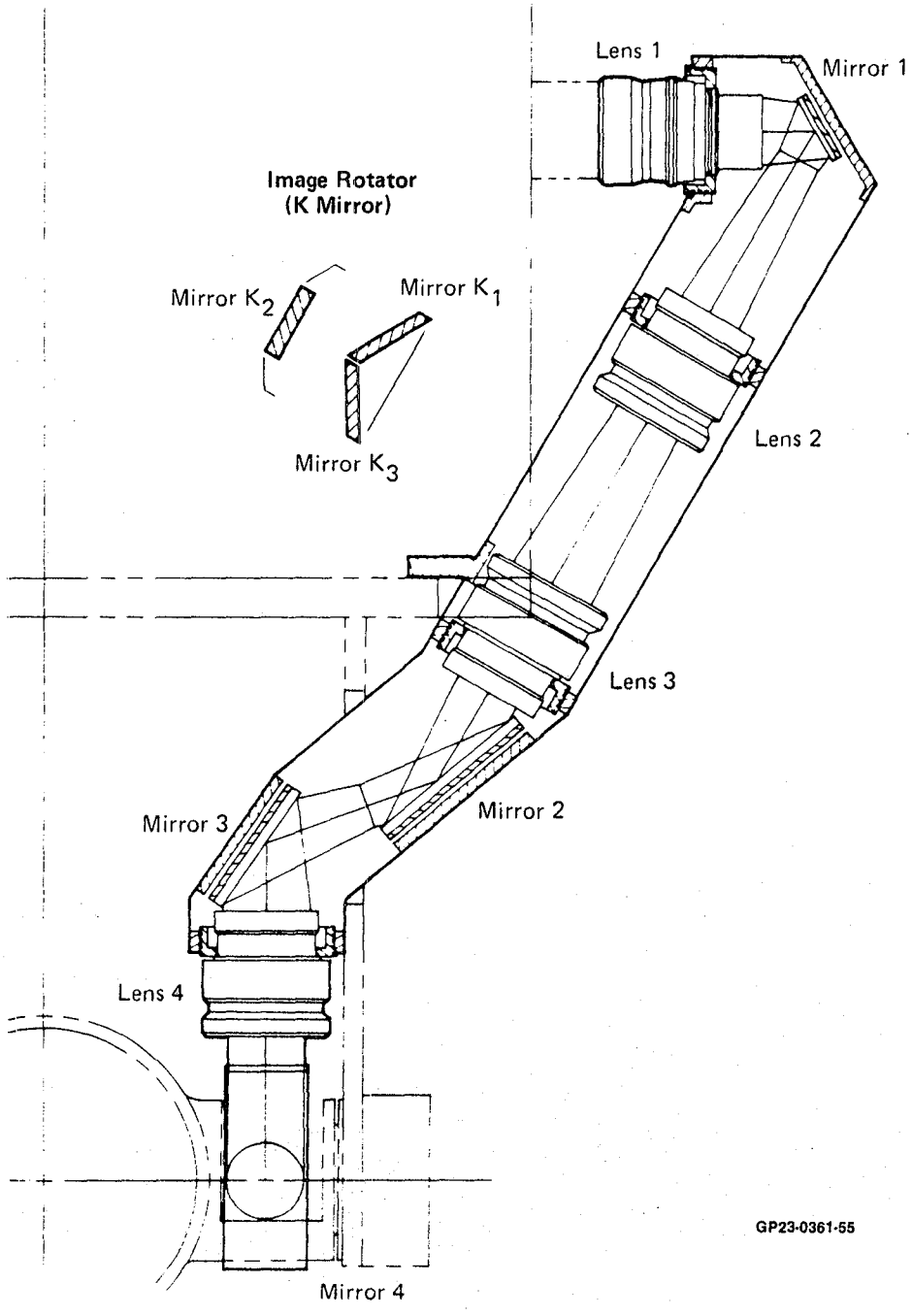

Figure 23-a. Relay Assembly

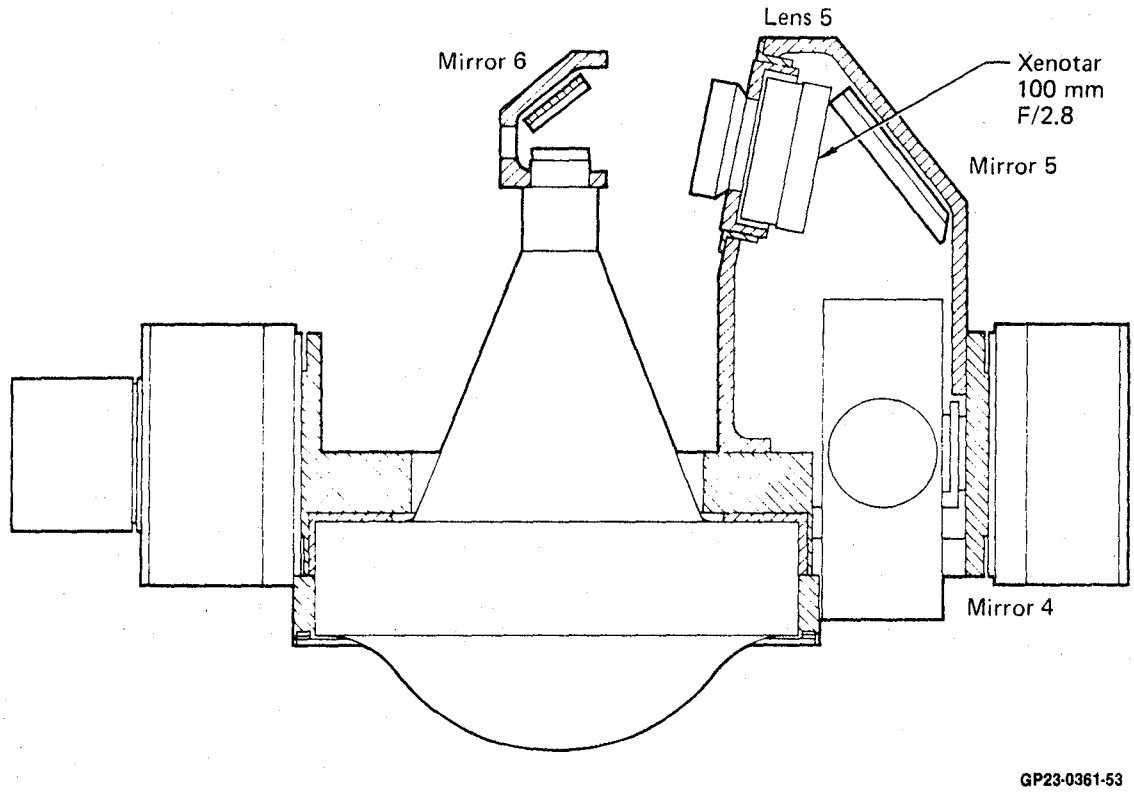

Figure 23b. Relay Assembly (Continued)

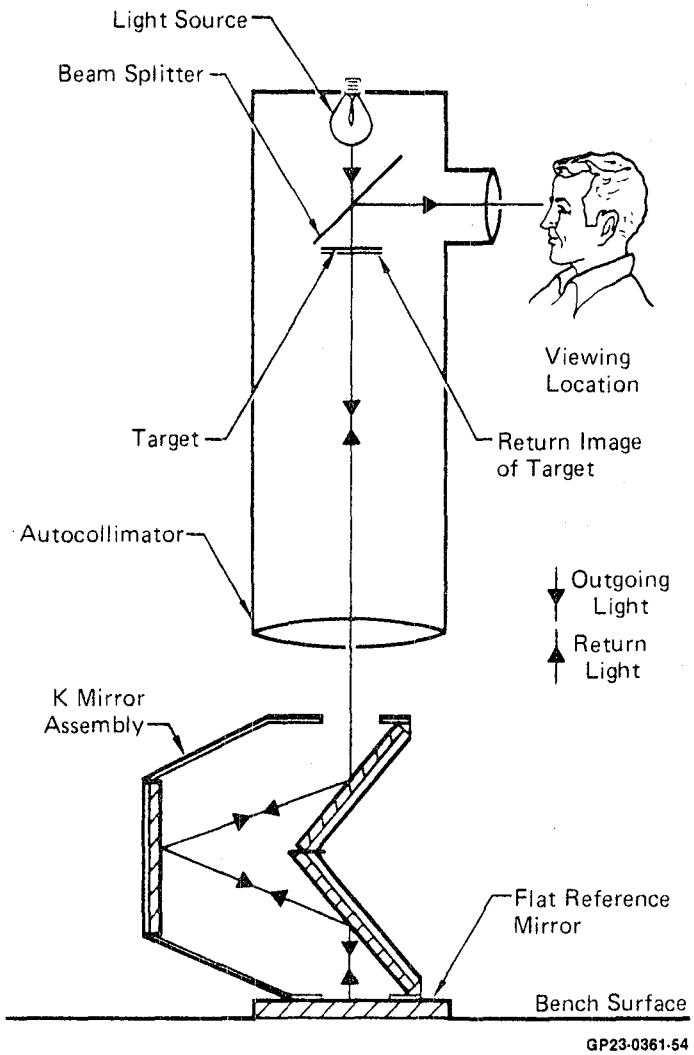

Figure 24. K Mirror Alignment Technique

3.2 DOME FABRICATION

A 9 ft. diameter dome was purchased from Spitz Corp. This consisted of 8 half gore shaped panels. The upper sections of the dome were assembled at MCAIR and modified to support the projector. Reinforcing was also added around the rear access opening. A photo of the assembled dome at EAFB was shown in Figure 2.

The NASA cockpit geometry was carefully measured and the projector located to give correct observer eye position, Figure 25. The dome sections were then modified to accommodate the projector and reinforcing was added along all exterior edges. A 3 view of the dome is shown in Figures 26, 27 and 28. A projector mounting ring was fabricated according to Figure 29 which installs in the dome as shown in Figure 30. The dome sections and mounting ring were then packaged for shipment to EAFB.

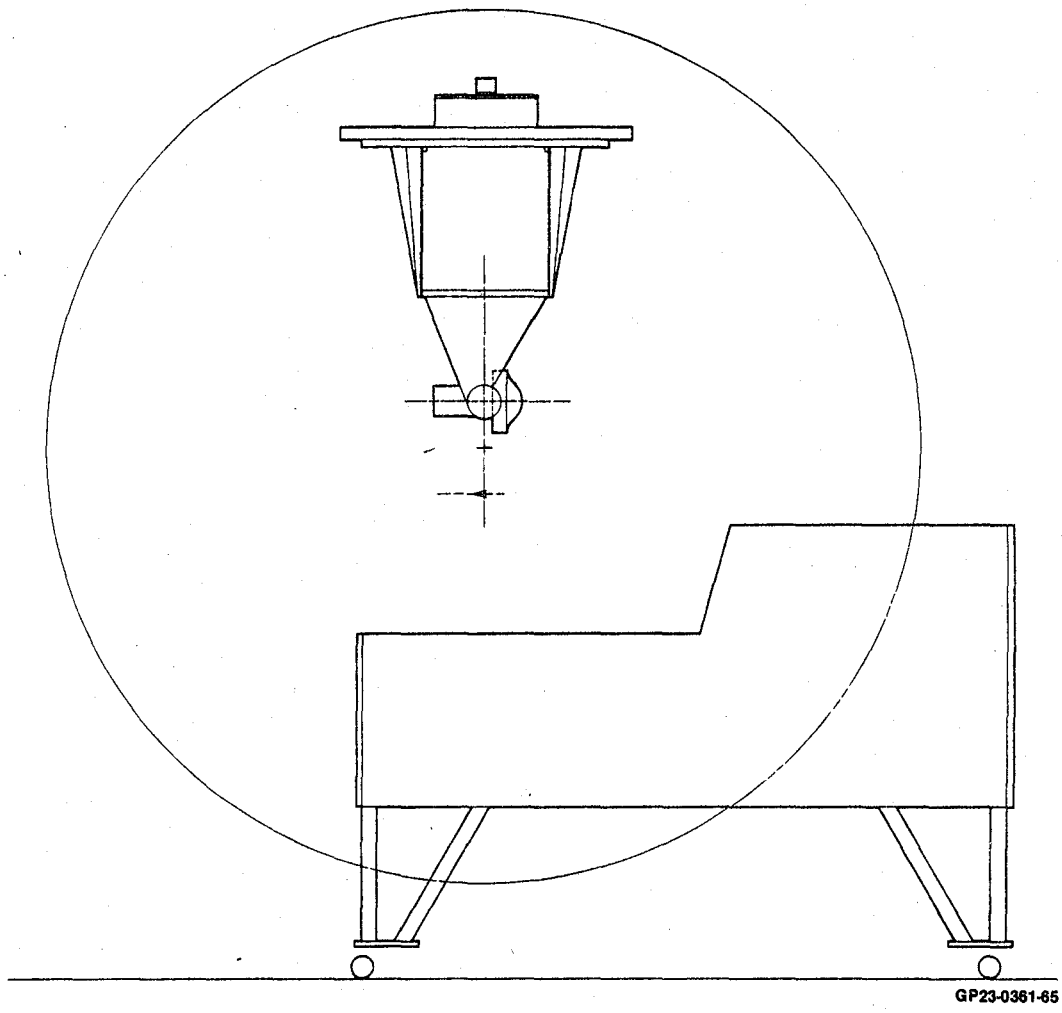

Figure 25. Cockpit/Projector Geometry

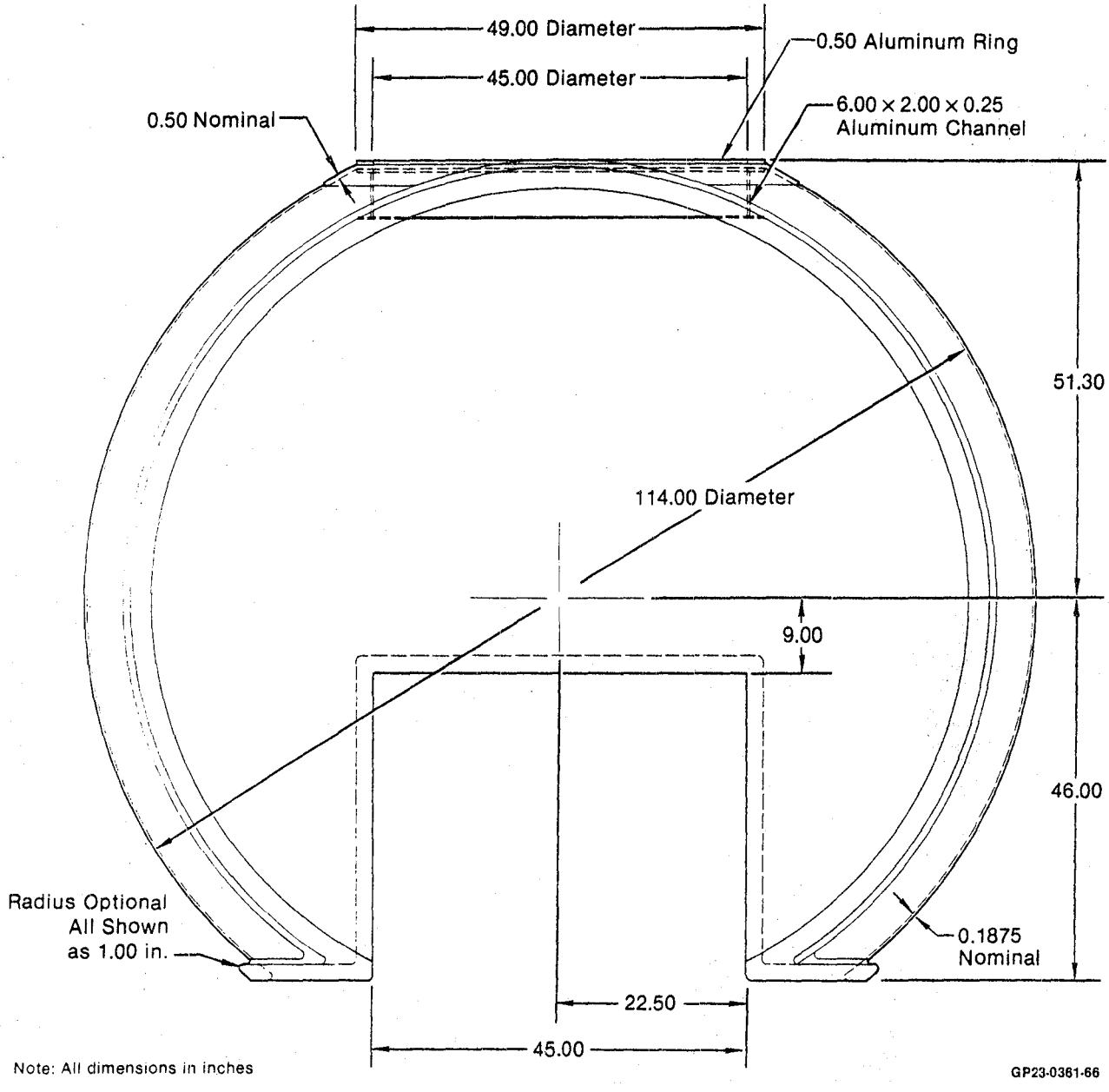

Figure 26. Dryden Dome - Front View

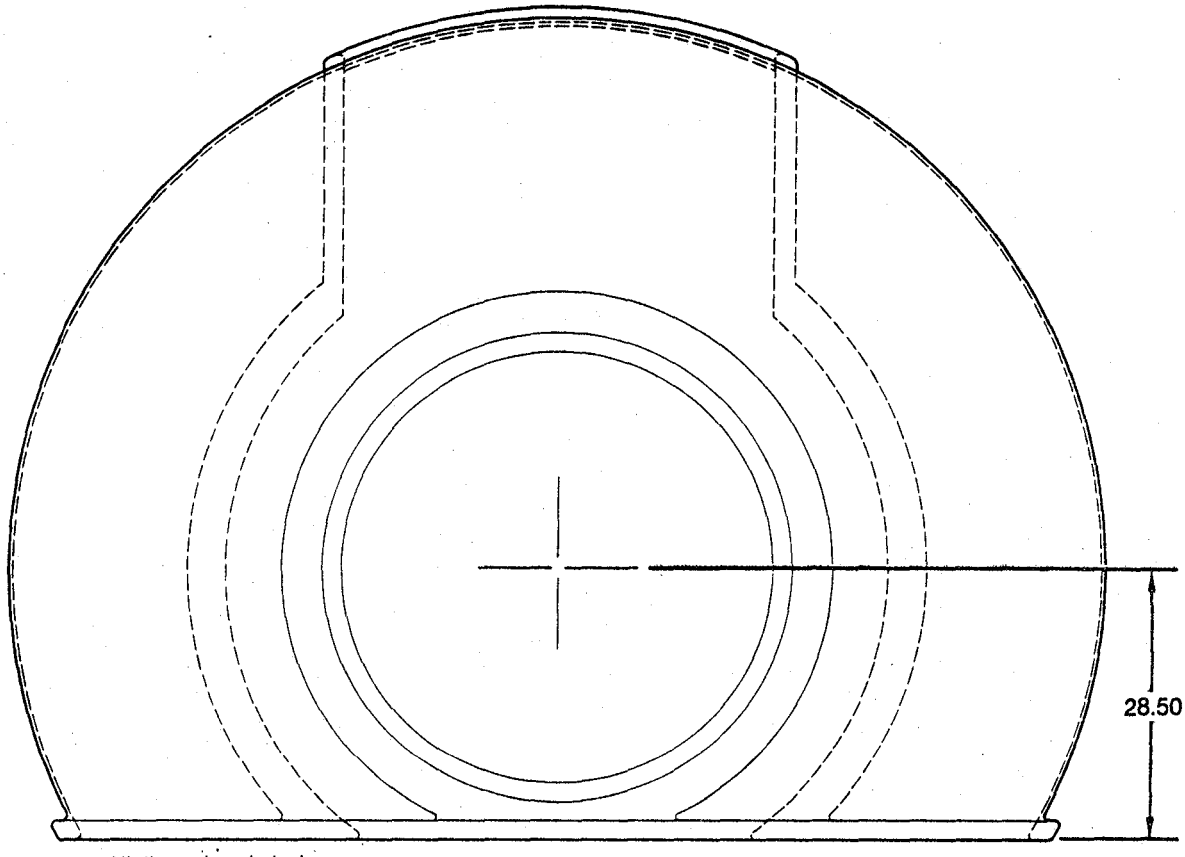

Figure 27. Dryden Dome - Top View

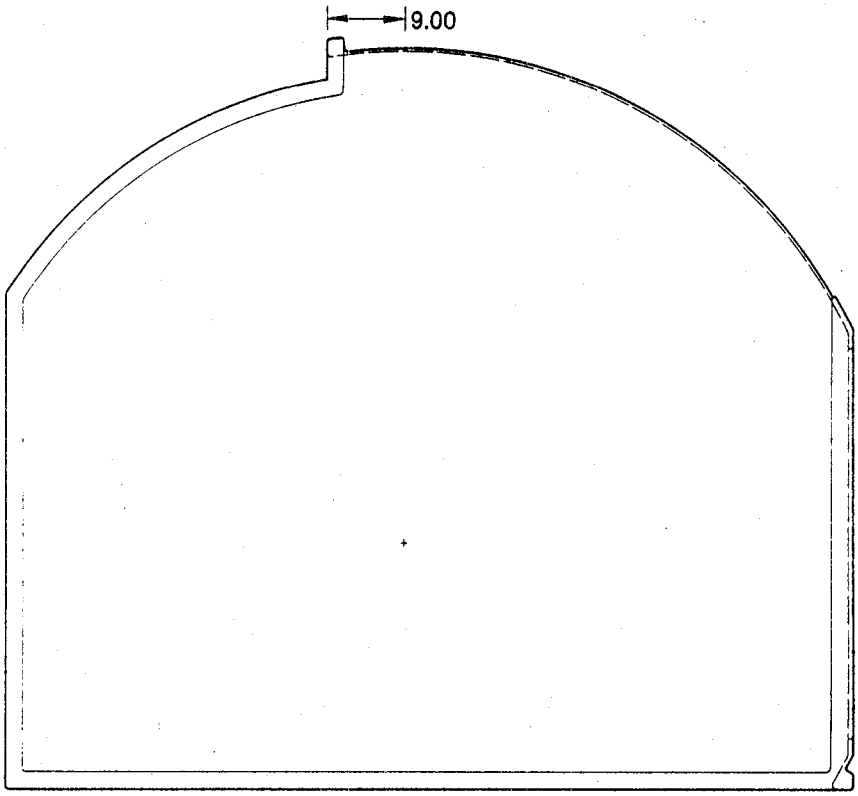

Figure 28. Dryden Dome - Side View

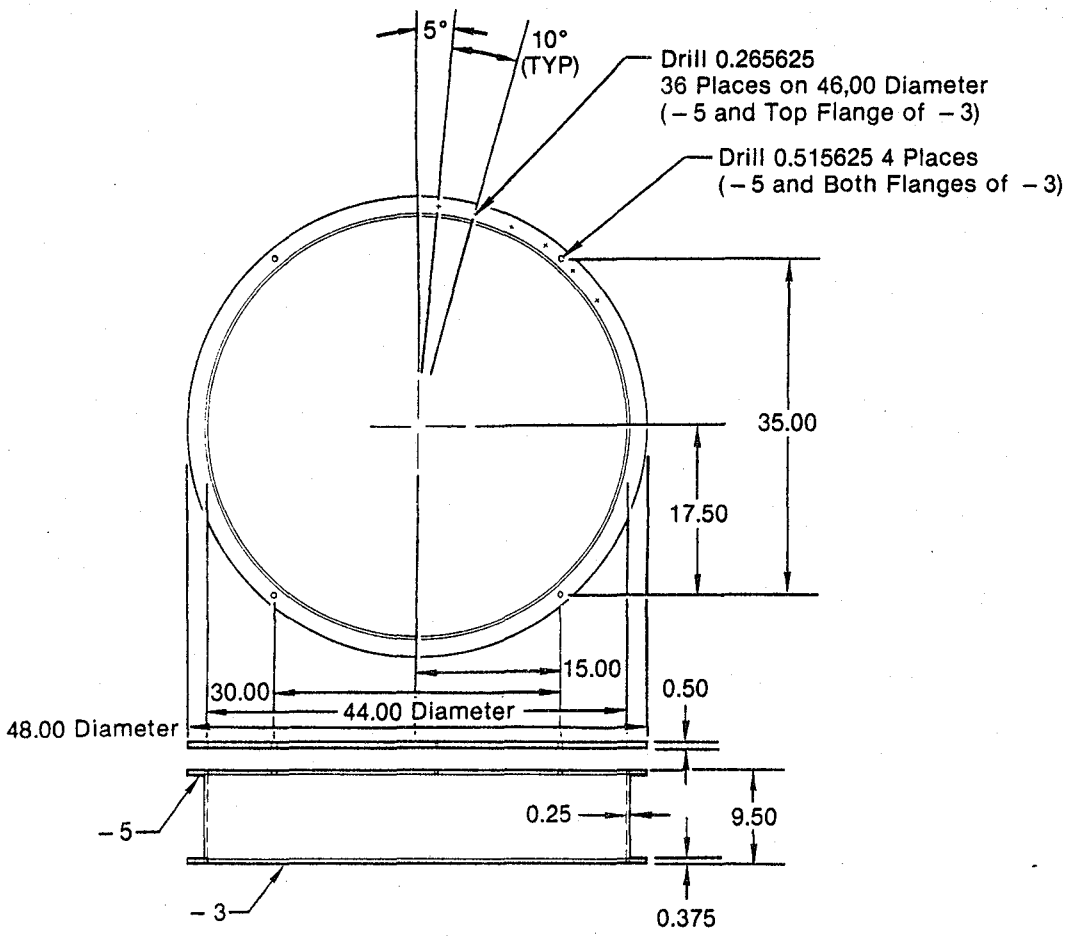

Figure 29. Projector Mounting Ring

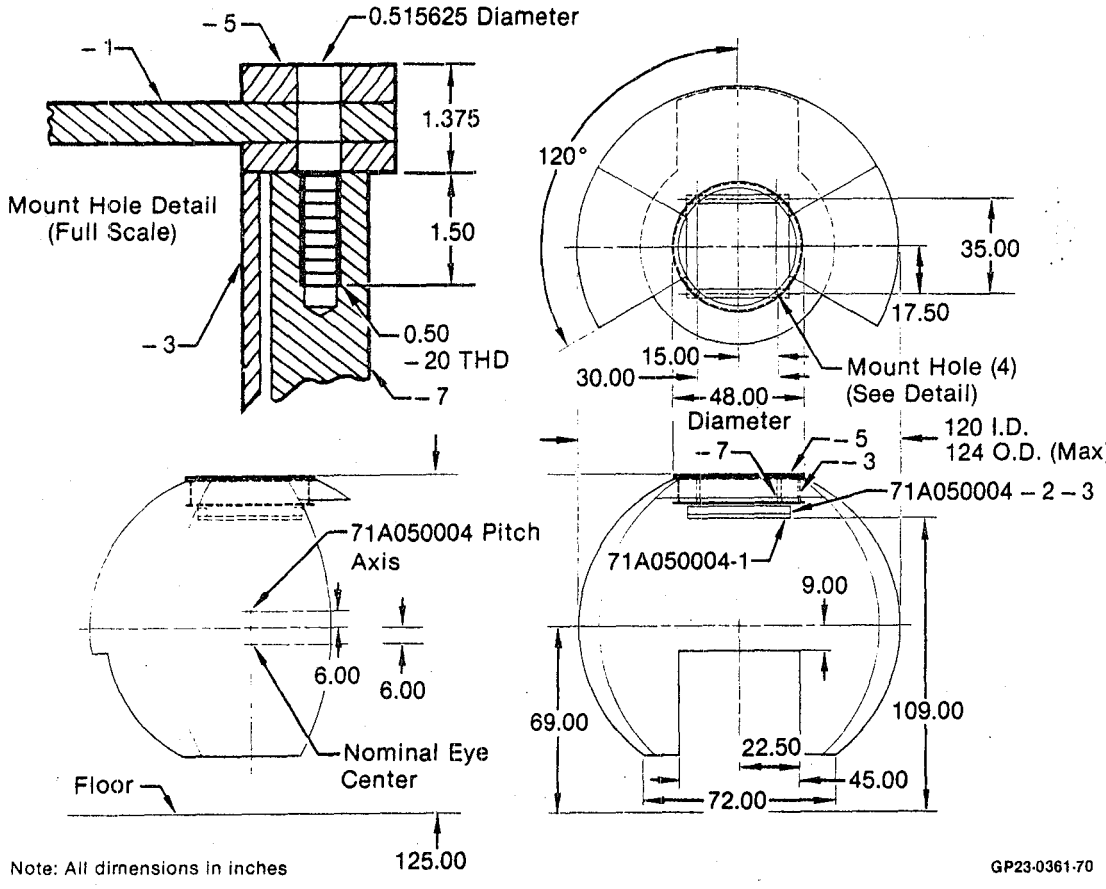

Figure 30. Dome Assembly

3.3 SENSOR MODIFICATIONS

The sensor modifications consisted of inverting the camera platform on the elevation gimbal, designing gimbal stops, and installing a new camera on the platform.

In order to gain better visibility over the cockpit sill, it was necessary to invert the camera platform so the lens was on the top. The inverted camera and the aircraft geometry are shown in Figure 31.

The PA30 installation required fixed aximuth gimbal stops and adjustable elevation gimbal stops. Azimuth stops were fabricated and installed inside the platform base. The adjustable elevation gimbal stop provide 0 to -5° of rotation and was designed to be accessible by the PA30 safety pilot. To make an elevation adjustment the lock plate screw is loosened and micrometer head is used to displace the camera. Then it is locked in the new position. These elements can be clearly seen in Figure 43 later in the report.

Installation of a new camera was thought to be necesary because the original GEC BE7073 camera was not flight qualified. The Edo Western 1430 series camera was the only flight qualified camera that would fit into our

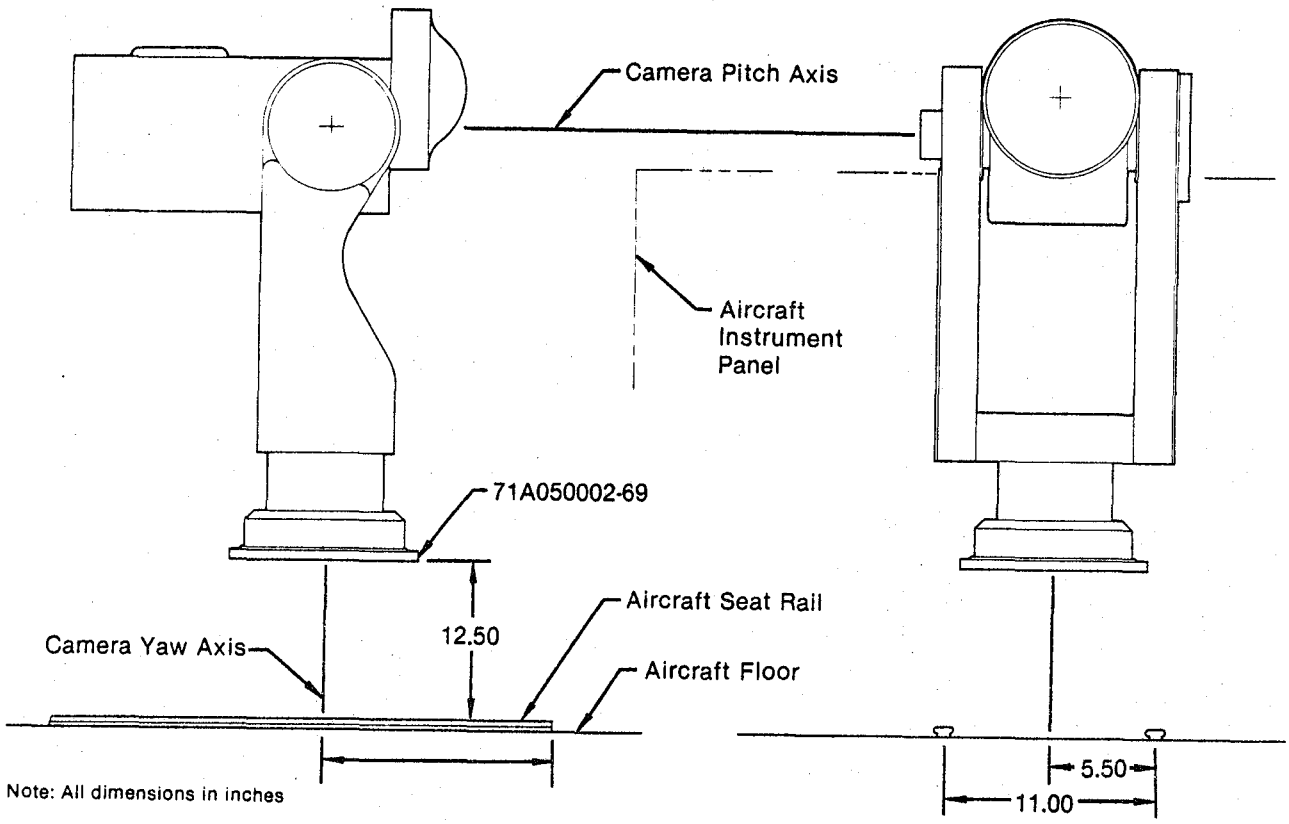

Figure 31. Inverted Camera Platform/Aircraft Geometry

sensor. Since it was advertised to have the same performance as the GEC camera NASA purchased the new camera. Mechanical installation of this camera was very easy-only requiring a new mounting collar. Achieving electronic compatibility however, proved to be another matter.

In order to get maximum resolution from the vidicon the circular image from the non-linear lens was scaled by the relay to be slightly smaller than the diode matrix which serves as the photo sensitive suface of the vidicon (Figure 32). In order to produce the desired raster a large overscan is required, i.e., the normal raster would fit well within the diode circle while ours is considerably larger. While the GEC camera had no problem functioning this way, the EDO Western camera scan could not be increased significantly. A co-operative effort was initiated with EDO Western to modify the horizontal and vertical deflection circuitry. While these modifications succeeded in increasing the deflection to the desired value - serious linearity and thermal drift problems resulted. The worst problem was a vertical linearity problem caused by coupling of the horizontal deflection signal into the vertical deflection yoke coil. This plus lack of horizontal linearity adjustment capability forced us to abandon this camera and return to the original GEC camera.

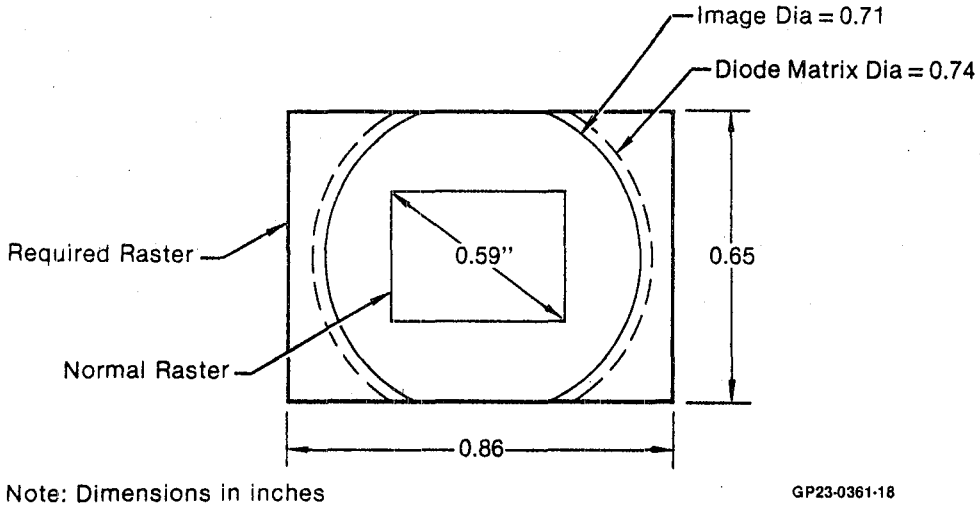

Figure 32. Vidicon Faceplate, Image and Raster Geometry

This Page Intentionally Left Blank

4. EQUIPMENT INSTALLATION AT NASA

After the above modifications the equipment was shipped to EAFB aboard a NASA DC3 aircraft. The primary MCAIR effort at EAFB was assembling and finishing the dome, projector installation, systems checkout, and calibration.

4.1 DOME ASSEMBLY AND FINISHING

The dome sections were bolted together and to the NASA fabricated dome support structure (Figure 25). After installing the projector mounting structure, the dome display surface was prepared and finished. This involved considerably more work than anticipated primarily because of imperfections in the dome panels and misalignments at the joints that become highly visible when the high gain aluminum display screen paint was applied.

After the final screen coating had dried the projector was installed. Figures 33 and 34 show the installation without the cockpit while Figure 35 shows the complete installation.

4.2 SYSTEMS TEST AND CALIBRATION

After separate functional tests on the sensor and projector they were coupled together and calibrated.

First the light value was aligned per its instruction manual for maximum light output and resolution with the optical relay removed as described in Section 3.1.1, Figure 22. Projector alignment was then checked per Table 1, Steps 3 to 9. When this was completed the projector and sensor were connected together for systems alignment. The procedures are described in Table 2. Rationale for these procedures are described below.

The objective of the alignment procedures shown in Table 2 is to obtain the best possible geometric registration between camera and projector. Some compromises must be made in this procedure because of distortion introduced by the focus corrector lens on the projector. This lens is required to focus the projection lens output on the dome surface (the non-linear lenses are designed to function at infinity focus). An additional lens element is required to reduce this to the 5 ft. dome radius). This lens, in accomplishing the required focus shift, introduces a distortion as shown on Figure 37. The 160° field of the sensor lens is displayed within about 146°. This distortion can be corrected to some degree by introducing magnification between camera image and projector object. (This can be easily done electronically by changing the size of the vidicon raster scan.) Results of this compensation are shown on Figure 38 for magnification of 2%, 5% and 10%. These data were calculated using the lens geometric transfer characteristics of Figure 39.

Originally we felt 5% magnification would be best because it results in very little distortion in the central 20° viewing cone. However, this reduces the sensor viewing capability of the system from 160° to about 120°. As experience was gained with the system central distortion was not as objectionable as expected and the minimum distortion system magnification of 2% will be acceptable. Here a peak error of about 2.5° occurs at 30° displacement. Sensor field of view capability is about 144° with this magnification which closely matches the display capability. It is quite possible that

TABLE 2. VARVS SYSTEM ALIGNMENT PROCEDURE

1. Locate the target, Figure 36, exactly 10 ft from the vertex (farthest forward point) of the nonlinear lens.
2. Point camera at target center. This is accomplished when horizontal and vertical radial lines are straight on the video monitor. (Make sure the target is normal to camera optical axis during this operation).
3. Point the projector so the target image lies on the intersection of the alignment strips on the dome. These strips are located as described in Table 4 for a 2% image magnification.
4. Adjust horizontal and vertical centering controls on the camera electronic unit until the horizontal and vertical radials are straight on the dome.
5. Check positions of the 10° and 15° circles in the dome with respect to the marks on the dome alignment bars. Adjust horizontal and vertical size controls on the camera electronics so the circles are centered on the marks. (Monitor both camera and projector pointing to make sure the radial lines remain straight on the video monitor and properly centered on the dome alignment bars during this operation).
6. In the event the circles can not be made to simultaneously lie on the marks on both sides of the center, linearity adjustments must be made. This must be an iterative adjustment because the linearity controls also affect centering and size. The best way is to rotate the linearity control a precise amount then recenter and resize the picture as described in 4 and 5 above - then note the magnitude and direction of the linearity change. Use this observation to anticipate magnitude and direction of the next change.

GP23-0361-16

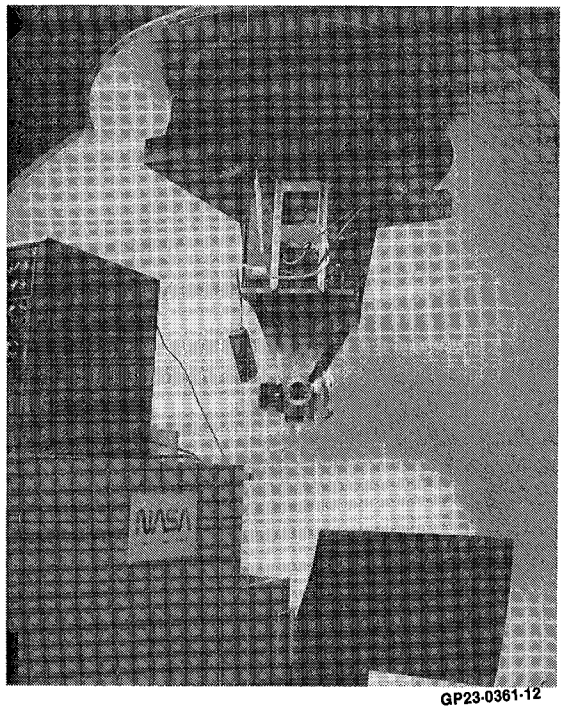

GP23-0361-12

Figure 33. Projector/Dome Assembly

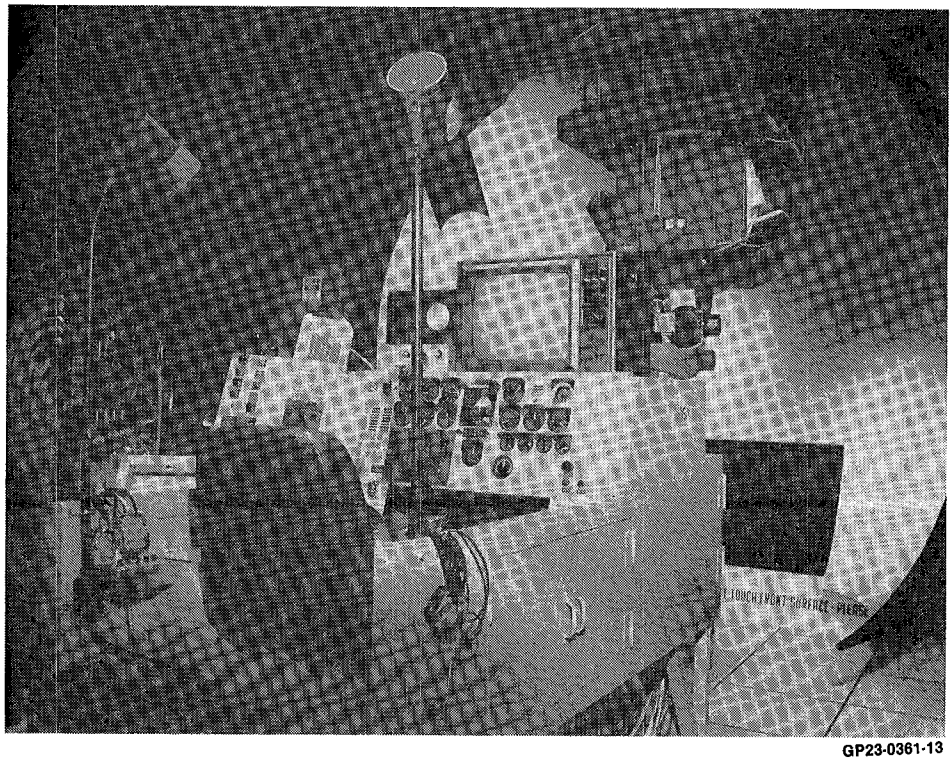

GP23-0361-13

Figure 34. Projector/Dome Assembly

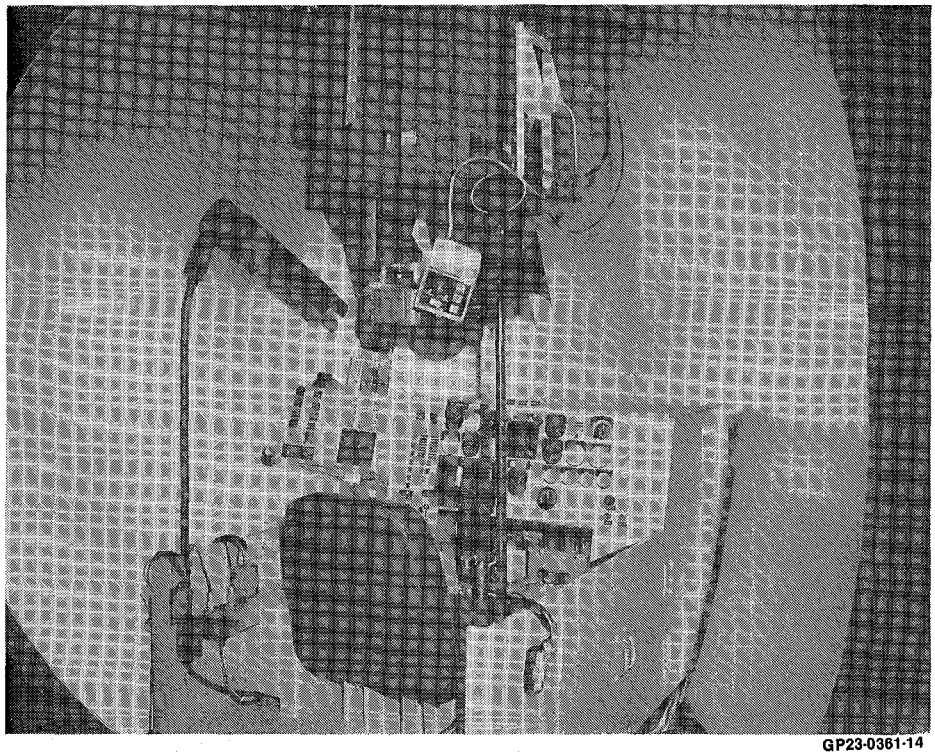

GP23-0361-14

Figure 35. Projector/Dome Assembly with Cockpit Installed

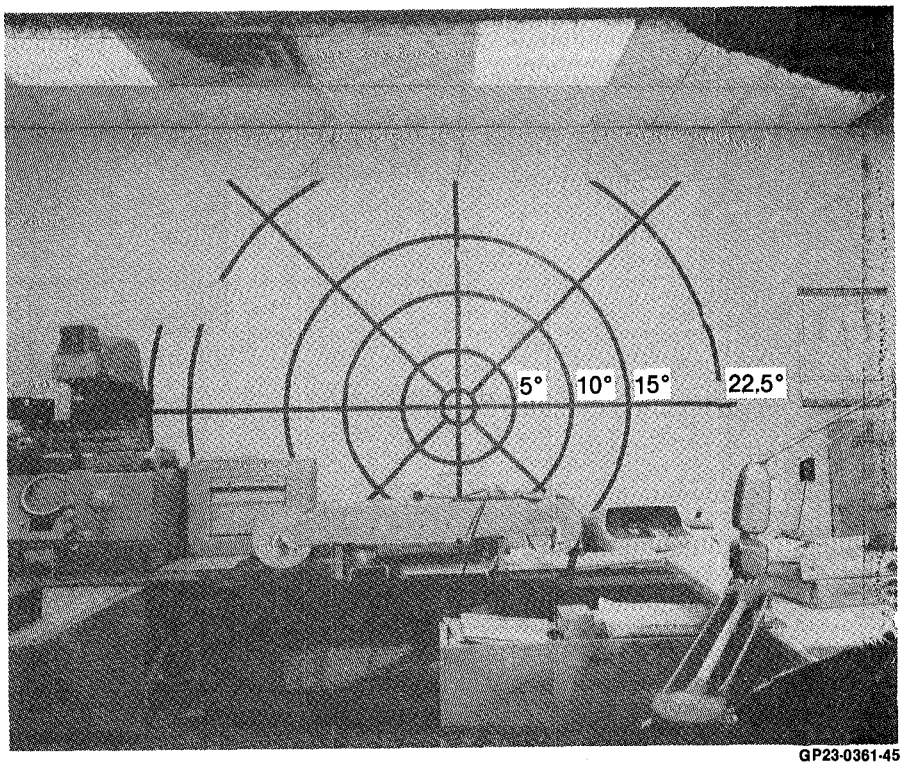

Figure 36. Circular Alignment Fixture

further experimentation may show that unity magnification is also acceptable. For this reason calibration procedures for unity, 2% and 5% are computed below.

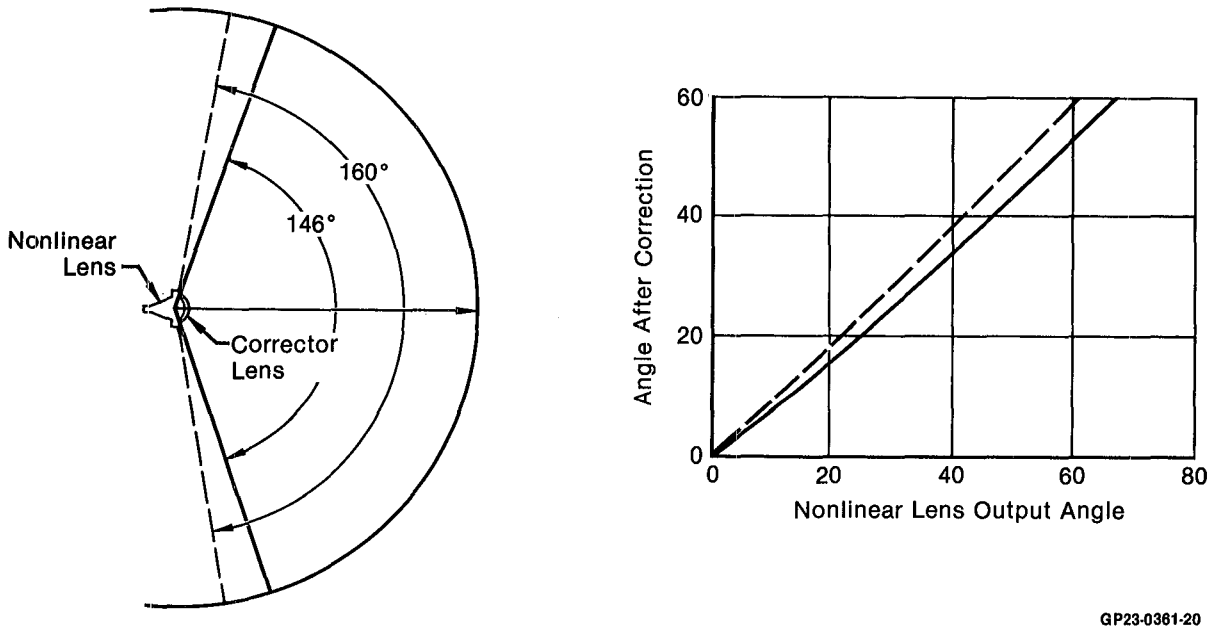

Figure 37. Geometric Distortion Introduced by Projector Focus Correction Lens

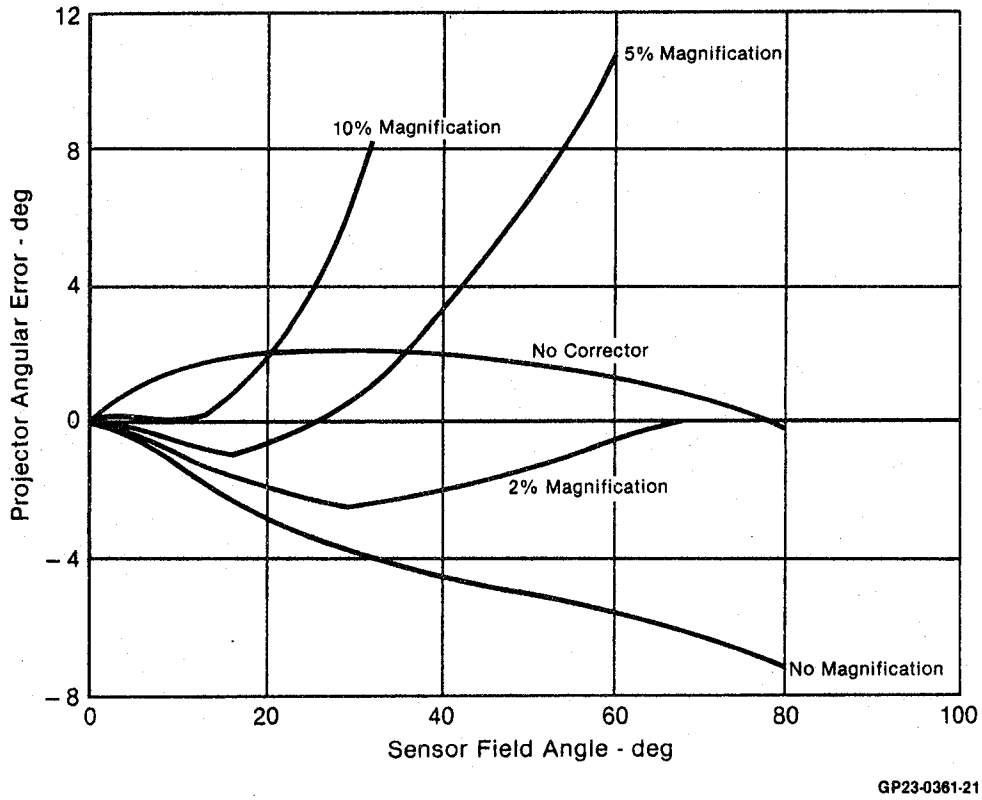

Figure 38. Total System Geometric Distortion

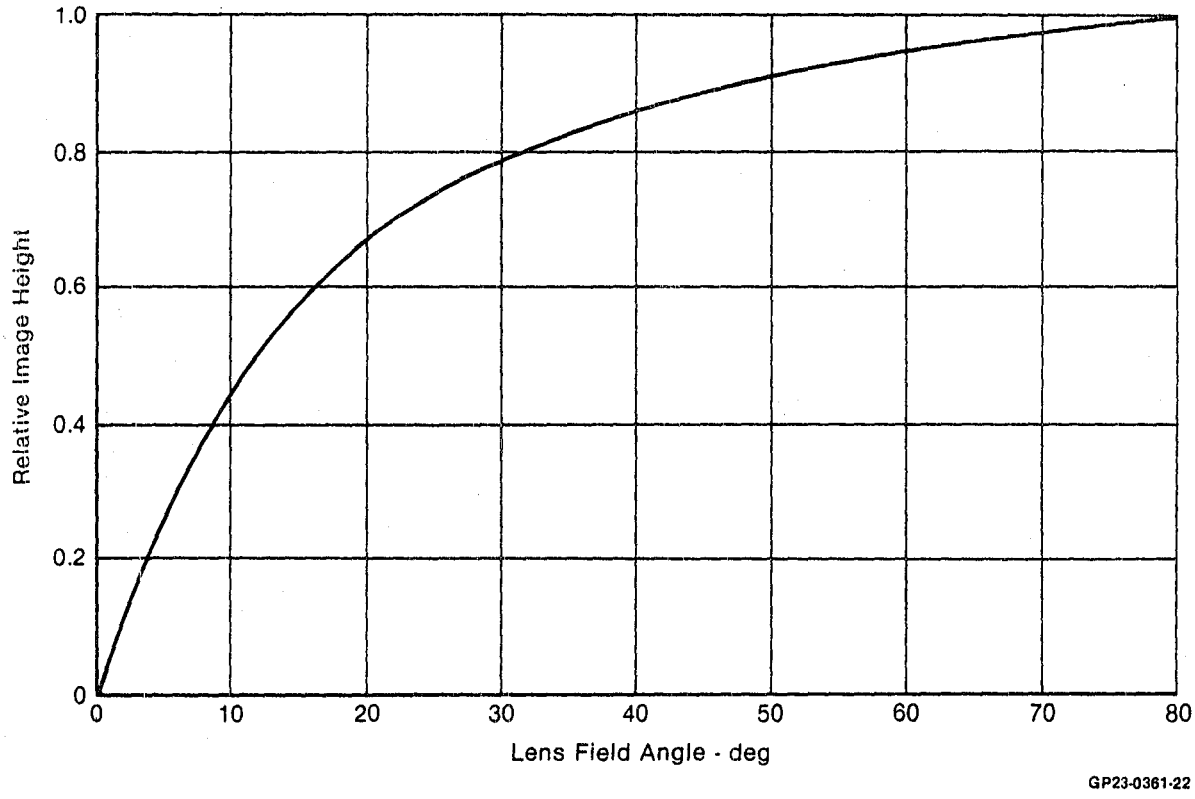

Figure 39. Nonlinear Lens Transfer Characteristics

When working with the alignment target of Figure 36 some additional errors must be considered. These are associated with the variable nodal point location within the non-linear lens (Figure 40) which varies the effective distance to the target from which camera angles are measured. For any particular viewing angle (field angle) the corresponding distance from Figure 40 must be added to the vertex to target distance in order to compute distance values on the target board, i.e., if a 15° field angle is desired the effective target distance is 10 ft. or 120 inches plus 9" from Figure 40 or 129". A 15° angle would therefore be generated by an object on the target board located

$$R = 129 \tan 15° = 34.57"$$

from the target center.

Unfortunately the actual target board circles were laid out assuming a constant 120" viewing distance, therefore they don't project the labeled angles to the camera. Table 3 shows the actual angles they project at a 10' vertex/target distance. Also shown on this table are the distances these labeled circles should appear in the dome image measured from the target center for the three magnification values under consideration.

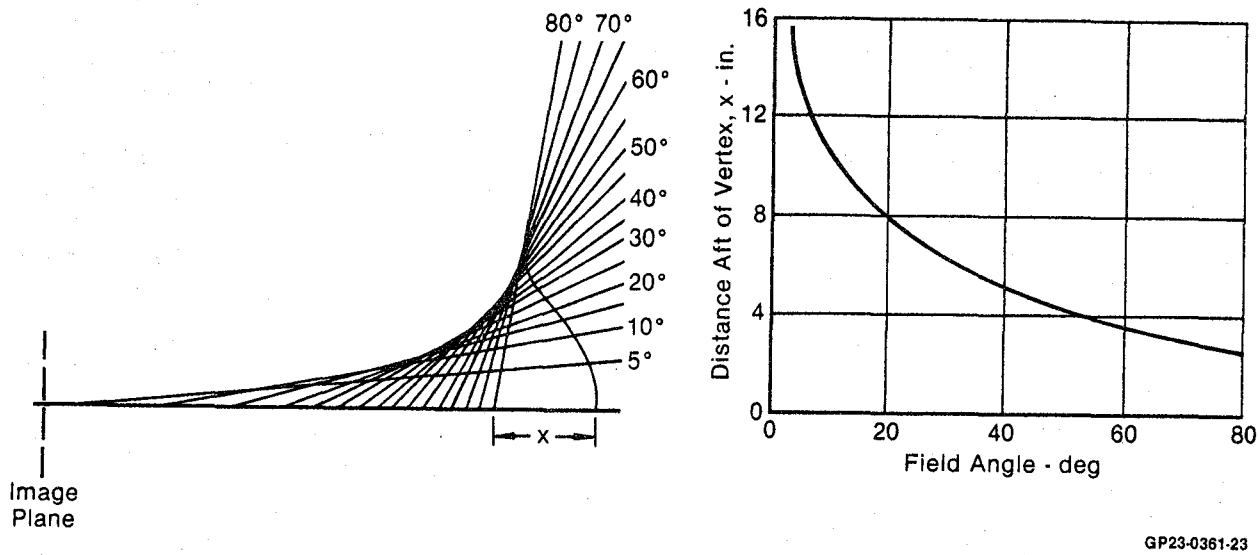

Figure 40. NLL Nodal Point Location

TABLE 3. SYSTEM CALIBRATION GEOMETRY

Target		Sensor		Display								
				0 Magnification			2% Magnification			5% Magnification		
Lable (deg)	Radius (in.)	Nodal Point Location (in.)	Lens Field Angle (deg)	Error (deg)	Projected Angle (deg)	Image Display (in.)	Error (deg)	Projected Angle (deg)	Image Display (in.)	Error (deg)	Projected Angle (deg)	Image Display (in.)
5.0	10.49	13.27	4.50	−0.60	3.90	4.08	−0.40	4.10	4.29	−0.30	4.20	4.39
10.0	21.16	10.74	9.18	−1.22	7.96	8.34	−0.94	8.24	8.63	−0.60	8.58	8.98
15.0	32.15	9.24	13.95	−2.10	11.85	12.41	−1.43	12.52	13.11	−0.95	13.00	13.61
22.5	49.71	7.60	21.38	−3.00	18.36	19.23	−2.00	19.38	20.29	−0.45	20.93	21.92
25.0	55.96	7.20	23.75	−3.20	20.50	21.50	−2.12	21.63	22.65	−0.20	23.55	24.66

GP23-0361-19

5. TEST AND RESULTS

5.1 GROUND TESTS

After calibration using a hard wire sensor/projector link, NASA suggested we evaluate the system when operating with their TV transmission and distribution system. For this test the sensor was installed in a NASA van that was equipped with a video data link. The sensor was mounted as far forward as possible on top of the engine cover so it could have maximum visibility out of the windshield. The sensor video was transmitted to the base tracking station just as it would operate in flight. The tracking station transmitted the video to the Dryden Flight Research Center receieving terminal where it was converted to composite video and routed to the RPV Lab through their normal video distribution system. The video was recorded at each end of the distribution system to evaluate any degradation. The van was driven around EAFB.

Except for an occasional drop out of the data link due to line of sight obscuration the video display was very good. Reception was noise free with no noticable degradation in dynamic range or bandwidth. The video tapes were excellent. They have become a standard for demonstrating the VARVS System to visitors.

5.2 FLIGHT TESTS

The sensor was then mounted in the PA30 aircraft. This installation is shown in Figures 41 to 44. Several flights were made for imagery evaluation (piggybacked on other PA30 missions). The only problem noted was in the exposure control system. Because of severe obscuration of the sensor field of view by the PA30 dashboard, the exposure system became almost as sensitive to dashboard illumination as to the outside world luminance. The problem can be seen in Figure 31. Whenever the sun illuminates the dash through the canopy the higher vidicon output forces the exposure control system to reduce it aperture which in turns causes the outside scene to become dark or underexposed. Conversely when the dark dashboard is fully shaded the exposure control opens up and overexposes the outside scene.

Since the object of the program was to evaluate the VARVS for RPV landings we calibrated the exposure system to operate best for the relative sun/aircraft/runway geometry during landing.

Only one RPV landing was flown with the VARVS. It was an excellent landing, however, the exposure control problem was apparent during approach when a cloud shaded the runway area. Since the dash was receiving normal illumination the sensor failed to open its aperature resulting in an underexposed scene. This was corrected, after a few anxious moments, by increasing the projector brightness output.

We attempted to correct the exposure problem by electronically restricting the portion of the vidicon format to provide exposure control. These are described in Appendix A. While this work was underway a decision was made by NASA to remove the sensor from the cockpit for safety reasons. NASA then asked us to consider an external installation, since this would eliminate the

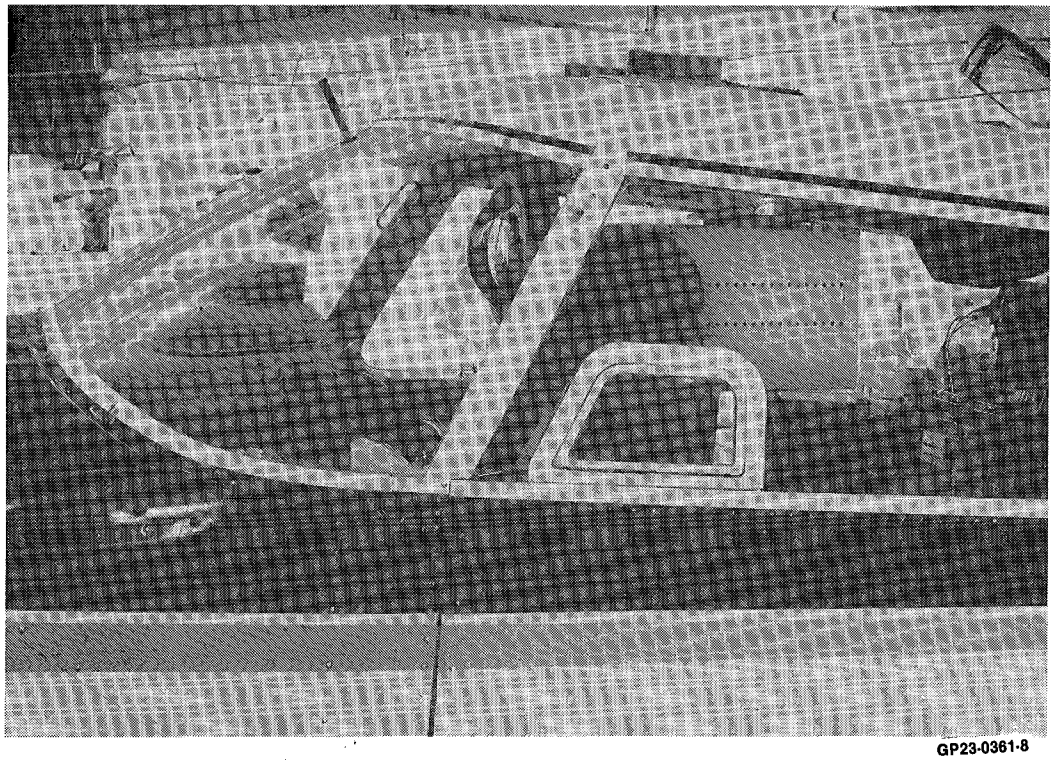

Figure 41. PA30 Internal VARVS Sensor Installation

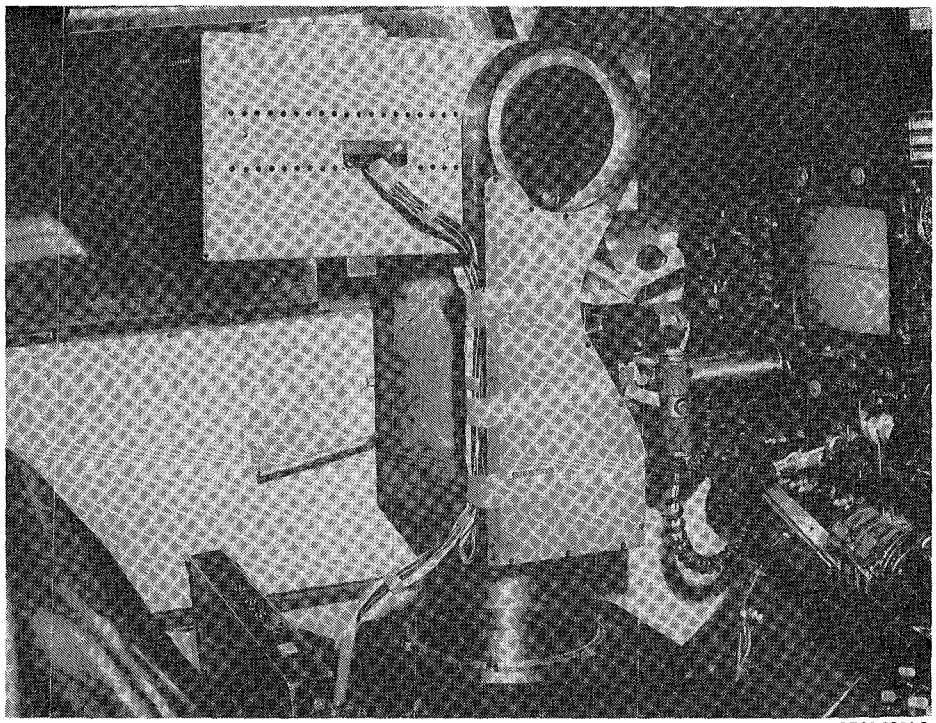

GP23-0361-9

Figure 42. PA30 Internal VARVS Sensor Installation

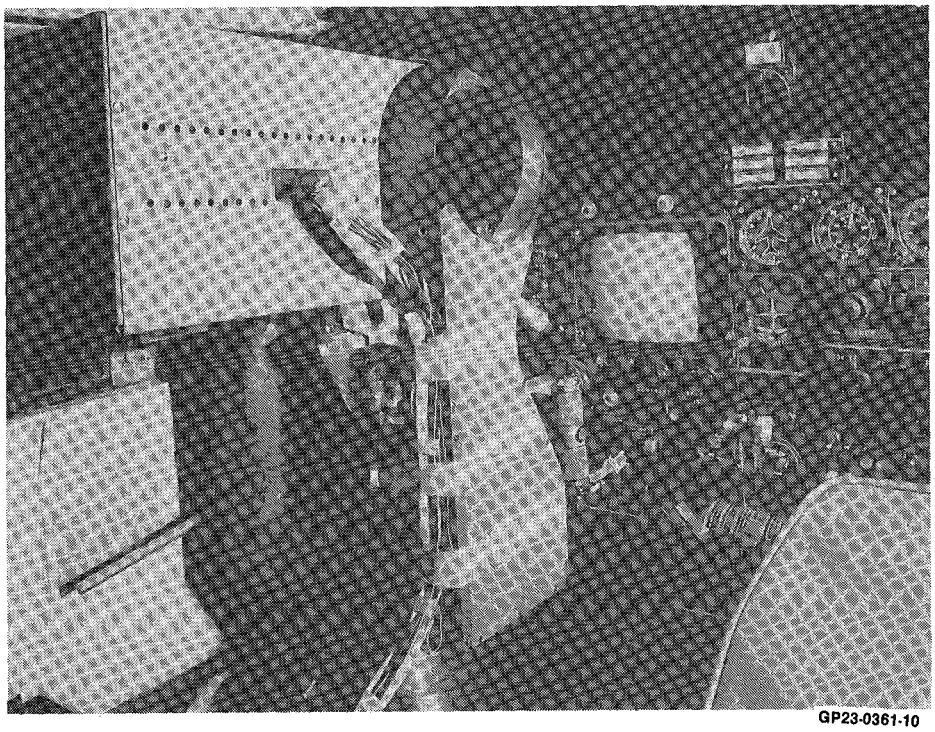

GP23-0361-10

Figure 43. PA30 Internal VARVS Sensor Installation

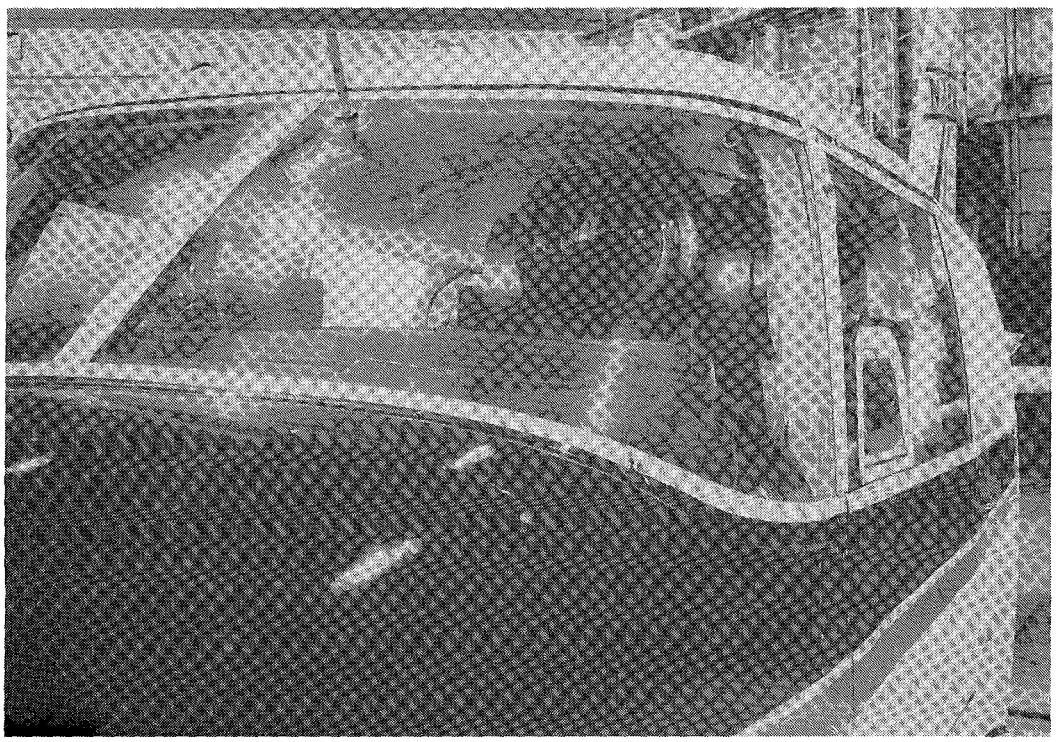

GP23-0361-11

Figure 44. PA30 Internal VARVS Sensor Installation

field of view obscuration that was causing the exposure problem. The external sensor installation was shown in Figure 1. Details of our effort on this installation are described in Appendix B.

The original camera electronics unit was misplaced during conversion to the external mount. We attempted to utilize the Edo Western camera (discussed in Section 3). To avoid the deflection and linearity problems previously discussed we put the camera back to its original configuration (small scan format) and reduced the image size on the vidicon faceplate by modifying the optical relay.

While this eliminated the deflection linearity problems discussed earier, it created additional problems that resulted in low resolution and poor exposure control performance. The resolution problem was expected because the image size reduction inherently makes the resolution cell size larger relative to the image size. This amounted to about a 50% loss in angular resolution which in itself made the display unacceptable for its intended use.

The exposure control problem resulted from the small area of the vidicon raster being used for imaging made its response to external light level changes very small (low gain). The resulting response deadband proved to be excessive. In an attempt to correct this, the light track module of the Edo Western camera was modified to allow independent adjustment of gain and level. However, when gain was increased sufficiently to reduce deadband, the system would oscillate. One flight was flown with the exposure control disabled and exposure manually set. The video display was very poor-particularly in resolution. The absence of light level control was also apparent.

This Page Intentionally Left Blank

6. CONCLUSIONS AND RECOMMENDATIONS

At termination of the contract no data had been taken on the original program objectives to evaluate the affects of a wide visual field of view on RPV control. We believe the primary cause of this was loss of program priority due to the retirement of Dr. William Winter early in the program. Later, when flight time was available, the camera electronic control unit was misplaced and has never been located. The only usable results are the video tapes from the van and early flights which can be used for laboratory demonstrations. Numerous such demonstrations have been made by NASA personnel. They have devised a very effective demonstration technique which involves first viewing the tape with the projector's field of view restricted to that of an equivalent bandwidth and resolution conventional TV system - approximately 15° x 20° (design of the field of view restricting devices are described in Appendix C). The full field of view (160°) is then demonstrated. Results have been very positive. The most significant observation has been the "realism" of the display, especially during dynamic situation such as take-off, landing, maneuvering, and low altitude flight. Apparently under these conditions, foveal vision plays a smaller role than the peripheral region. As a result the variable acuity nature of the display is hardly noticable. It appears one can determine altitude, attitude and speed much quicker and more accurately with the VARVS display than with a conventional TV display. This could be the result of visual integration over the human's entire field of vision.

These observations have suggested use of the display for flight simulators. Some work has been done on this application under MCAIR IRAD. This is discussed in Appendix D.1.

6.1 RECOMMENDATIONS

The results of the early tests have been sufficiently positive to justify purchasing a new camera for the VARVS program to permit completion of the original objectives of the program.

Also the potential of the VARVS display for simulator applications is additional incentive to continue development. The VARVS display requires only a single 525 line TV channel to generate its 160° field of view compared to 3 to 5 channels for conventional simulator visual displays. The result could be a sizeable cost reduction for many simulator functions.

This Page Intentionally Left Blank

APPENDIX A

EXPOSURE CONTROL MODIFICATIONS

The exposure problem was observed during initial flights. This problem is inherent in the pilot seat location of the sensor. The major contributor was solar illumination of the aircraft instrument panel which occupied about 30% of the vidicon image area. If the sun directly iluminated the panel the camera would "stop down" to the point where the outside world couldn't be recognized. Conversely if the panel was shaded the outside scene would become over exposed or "washed out". To correct this we designed a circuit that would electronically block the area of the camera vidicon occupied by the instrument panel. This circuit is shown in Figure A-1. This circuit allows any rectangular area of the vidicon to be used for exposure control, as shown in Figure A-2.

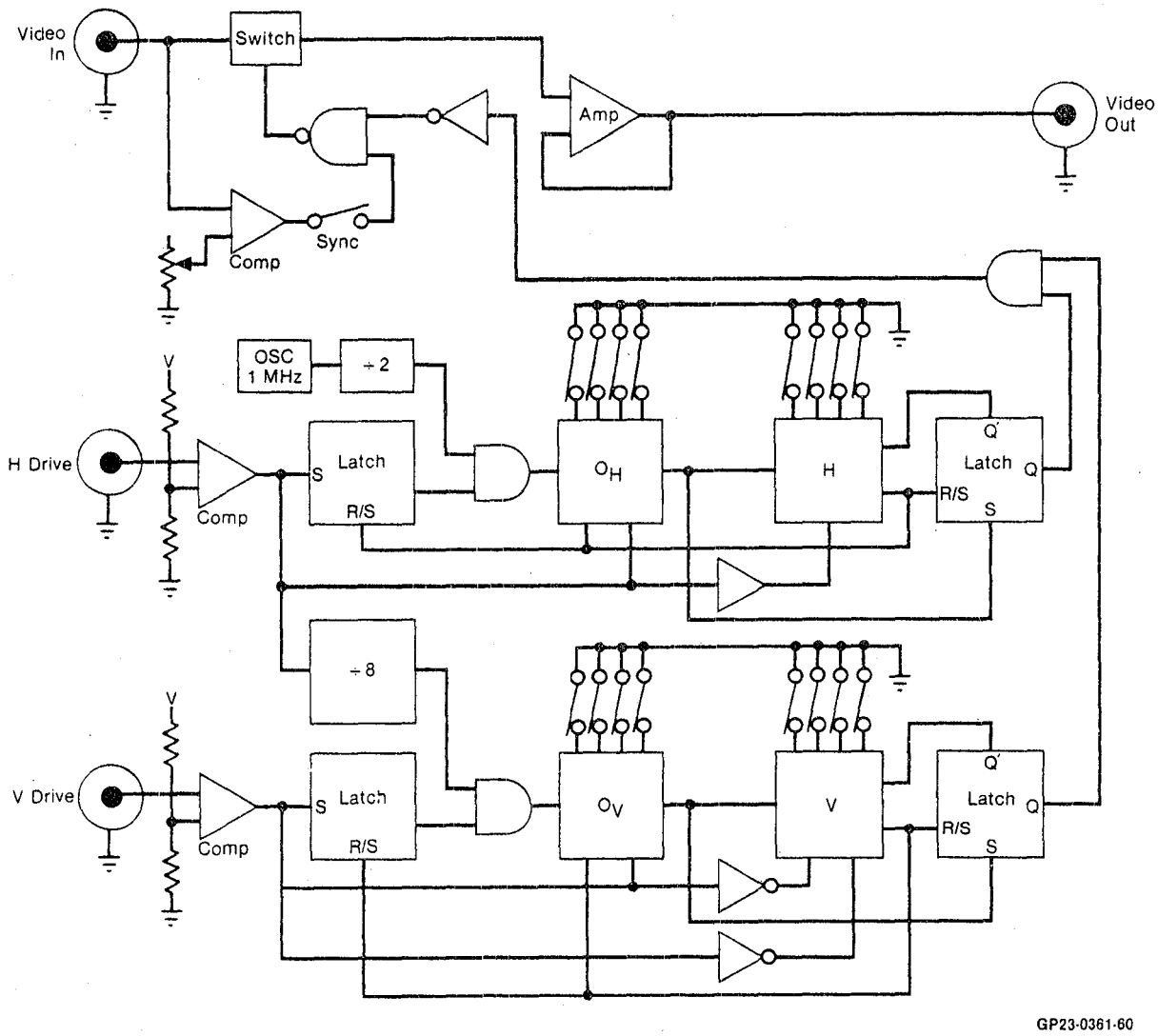

Figure A1. Initial AEC Control Circuit

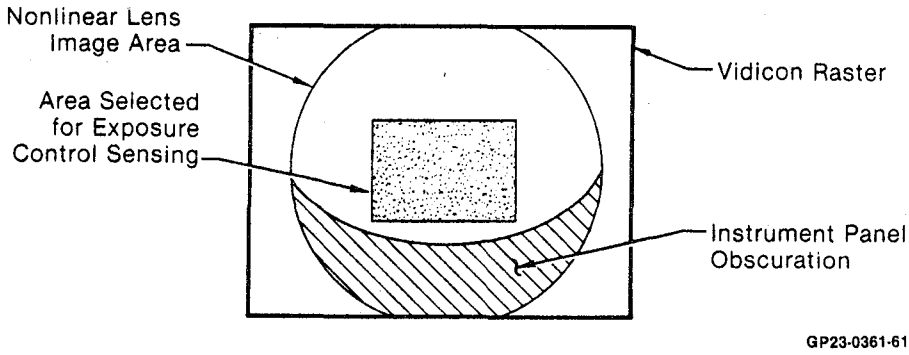

Figure A2. Vidicon Image Geometry

The selected area can be shifted anywhere on the vidicon by BCD switch sets (O_H) and (O_V). The size of the rectangle is controlled by BCD switches (H) and (V).

The circuit of Figure A-1 was constructed and tested. While it worked properly, it become apparent it would not function in the aircraft environment - apparently because of electrical noise and mechanical vibration.

The tests on the circuit had shown that a much simpler sampling format, shown in Figure A-3 would work just as well and would have considerably less video noise problems.

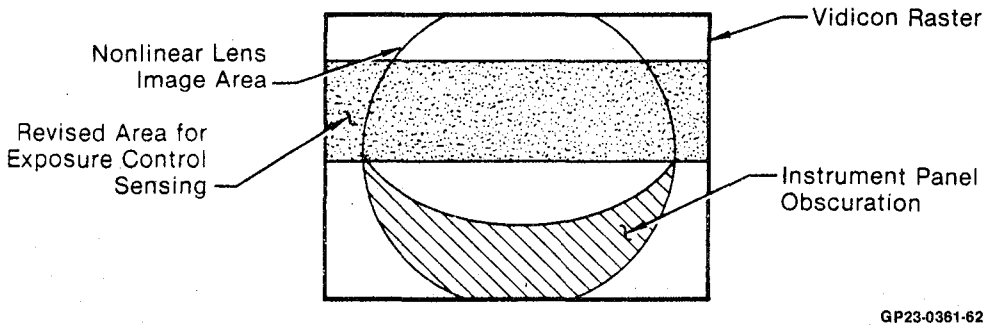

Figure A3. Revised Sensing Area for Exposure Control

A much simpler circuit was now possible (Figure A-4). This circuit was fabricated and installed in the PA30 aircraft. It was never used, however, because the safety pilots decided the visual obstruction caused by the camera location inside the cockpit was detrimental to flight safety.

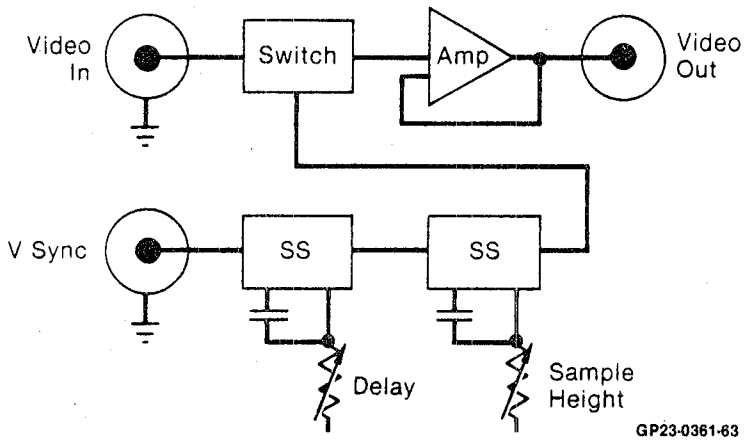

Figure A4. Revised Exposure Control Circuit

This Page Intentionally Left Blank

APPENDIX B

EXTERNAL SENSOR MOUNT

The sensor installation in the cockpit creates two problems. First the internal camera interfers with the safety pilots field of vision. Also the sensor field of vision is seriously limited by the dashboard, and dash mounted equipment (See Appendix A). For these reasons NASA asked us to determine the feasibility of an external camera mount. We determined the only location possible was on top of the canopy using the rails originally installed on the aircraft for a stereo camera system. A mount and fairing was then designed as shown in Figure B-1. This design centers around a dome which was purchased surplus by MCAIR several years ago. Approximately 1 inch had to be removed from its equator using a diamond saw. The remainder of the design was concerned with picking the proper mounting points. NASA refined the design and fabricated the mount and fairing. The installation less the fairing is shown in Figures B-2 through B-5 and the final configuration with fairing is shown in Figures B-6 through B-8.

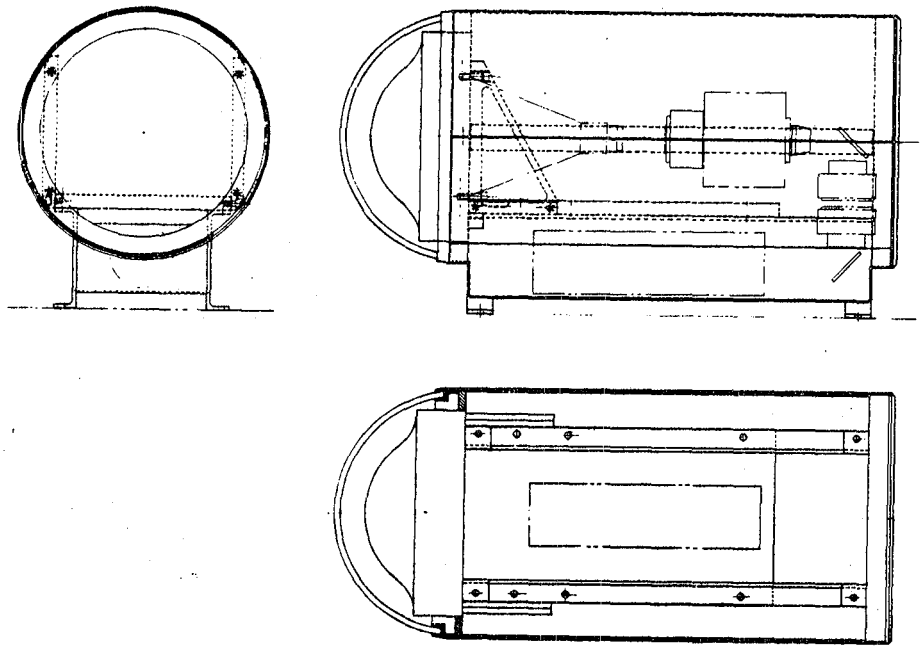

Figure B-1. External Sensor Mount Initial Design

GP23-0361-1

Figure B-2. PA30 External VARVS Sensor Mount

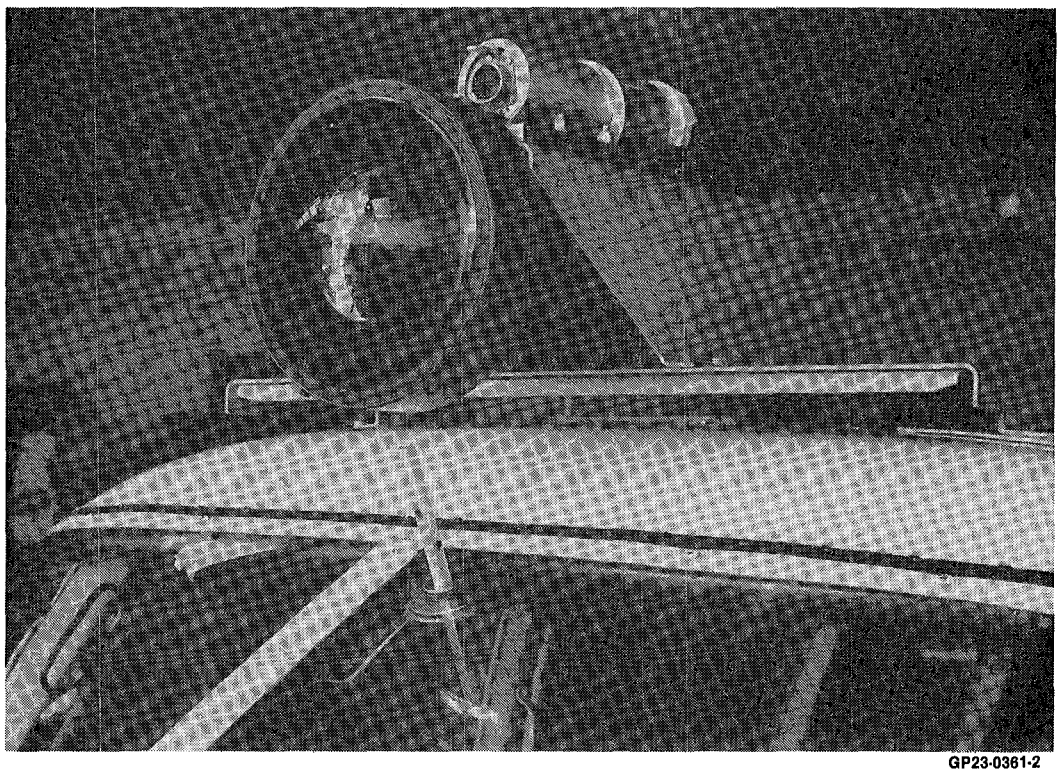

GP23-0361-2

Figure B-3. PA30 External VARVS Sensor Mount

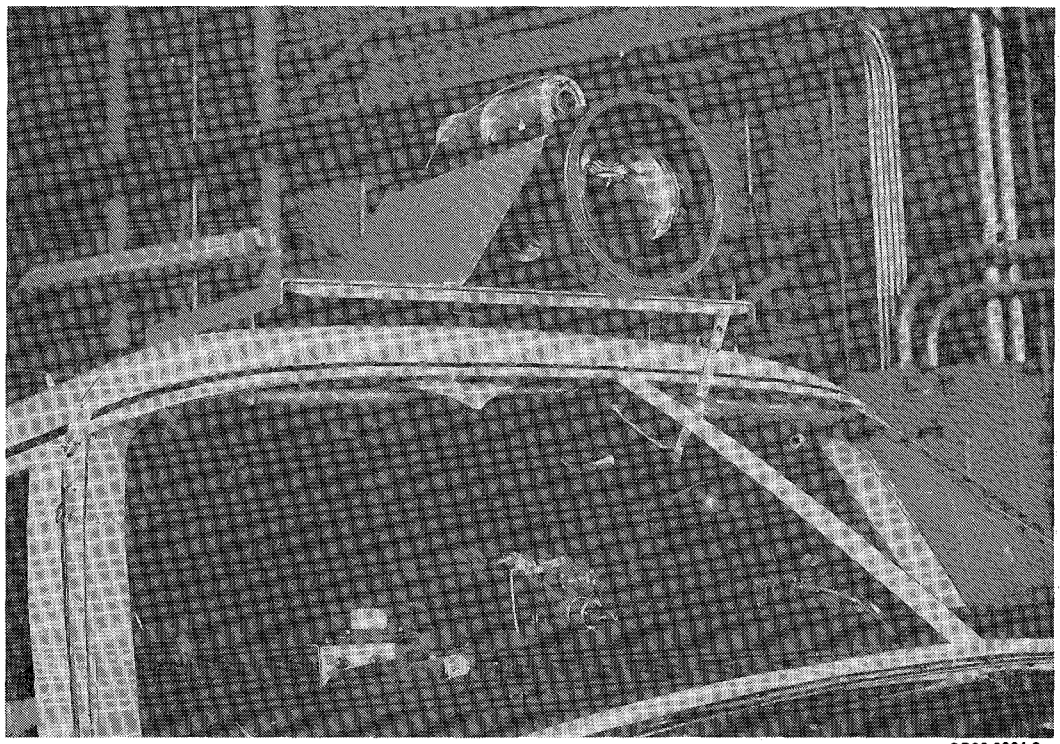

GP23-0361-3

Figure B-4. PA30 External VARVS Sensor Mount

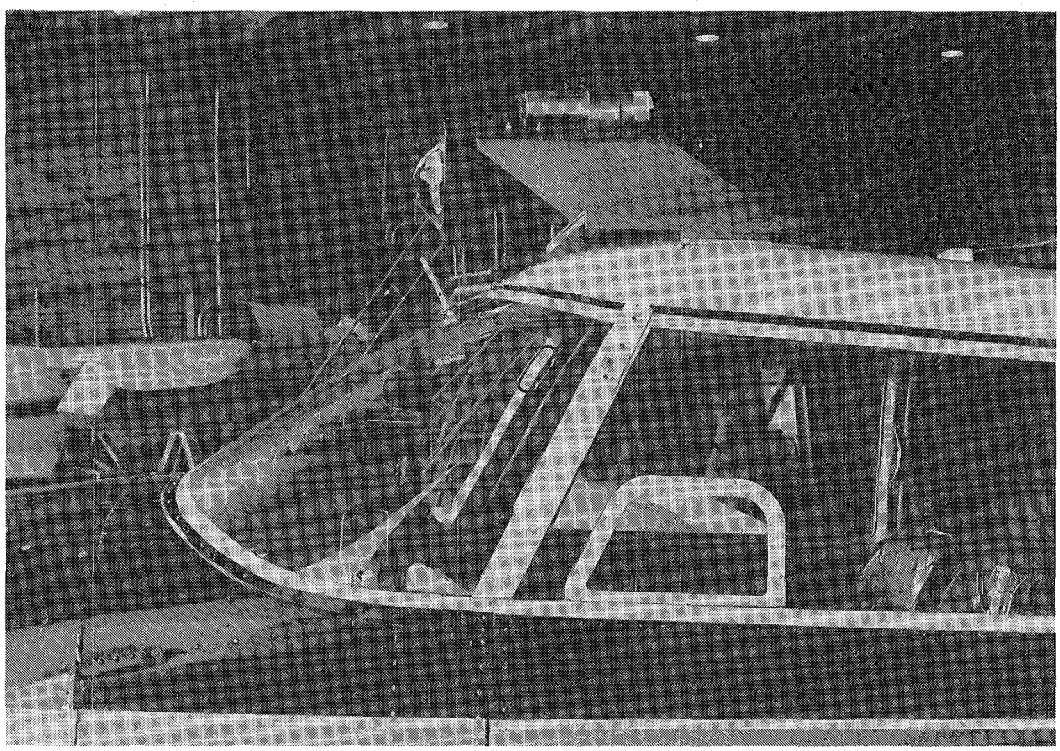

GP23-0361-4

Figure B-5. PA30 External VARVS Sensor Mount

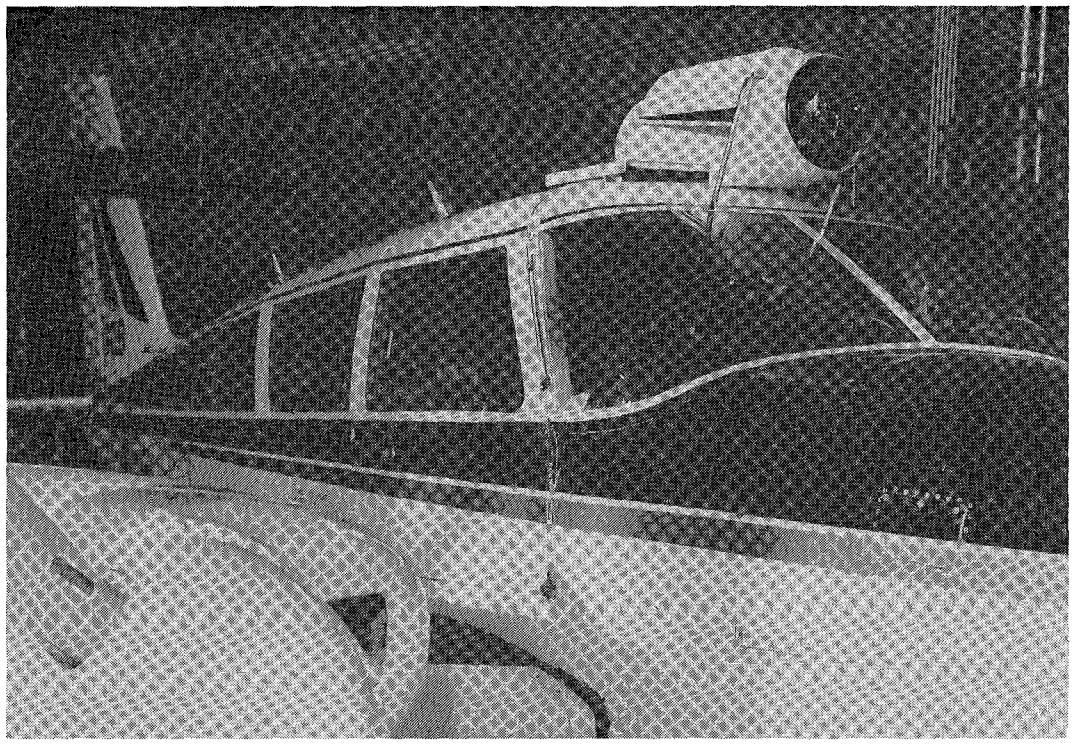

GP23-0361-5

Figure B-6. PA30 External VARVS Sensor Installation

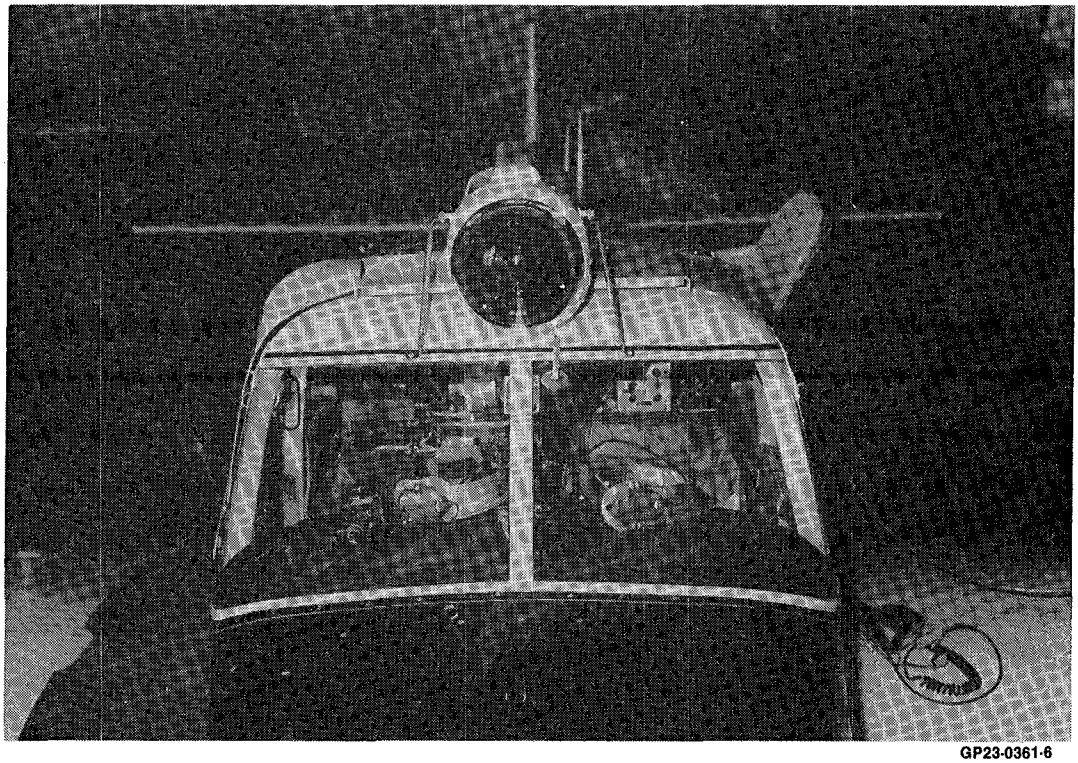

GP23-0361-6

Figure B-7. PA30 External VARVS Sensor Installation

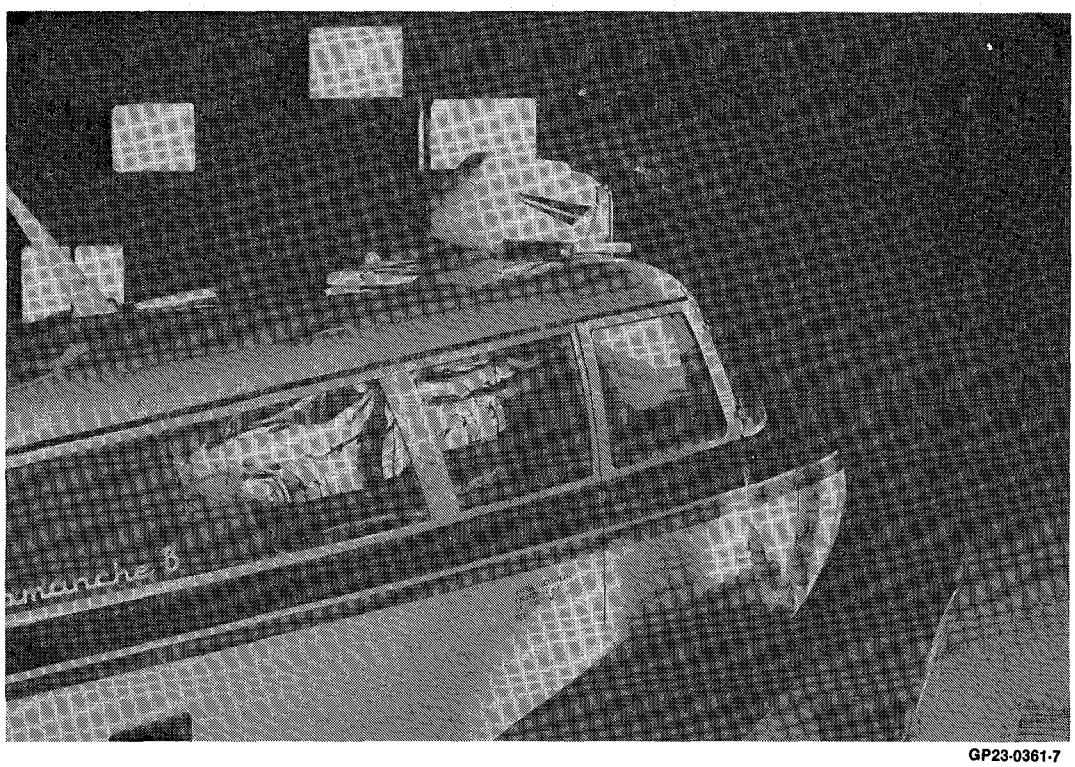

GP23-0361-7

Figure B-8. PA30 External VARVS Sensor Installation

APPENDIX C

PROJECTOR FORMAT MASK

Early in the program NASA conceived the idea of restricting the field of vision during demonstrations to that of an equivalent resolution conventional TV-approximately 15° x 20° and then removing the mask to show added information gained by the wide field. Initially we cut a hole in the lens cap of the projector to restrict the view.

After the cockpit was installed NASA found that the mask was very difficult to install and remove. They inquired if this could be done elsewhere in the system. We found this could be accomplished at the final image location in the relay. In fact, we had provided an opening in the relay housing for a filter, so the effort consisted of designing and fabricating the mask and mount. In order to project a rectangular field, a mask in the nonlinear lens image plane must be far from rectangular. It must be designed point by point using the nonlinear lens design equations. The result is shown in Figure C-1. The mask was cut out of brass and mounted in the assembly shown in Figure C-2. Sufficient clearance was allowed in the mask mounting holes so it could be initially aligned with respect to its support structure and then tightened in position so it will be aligned whenver the support frame is inserted into the relay.

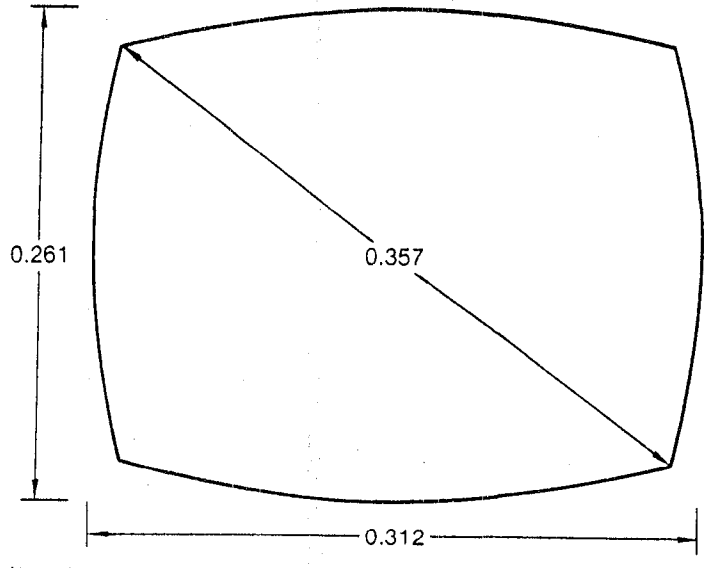

Figure C-1. Format Mask Geometry

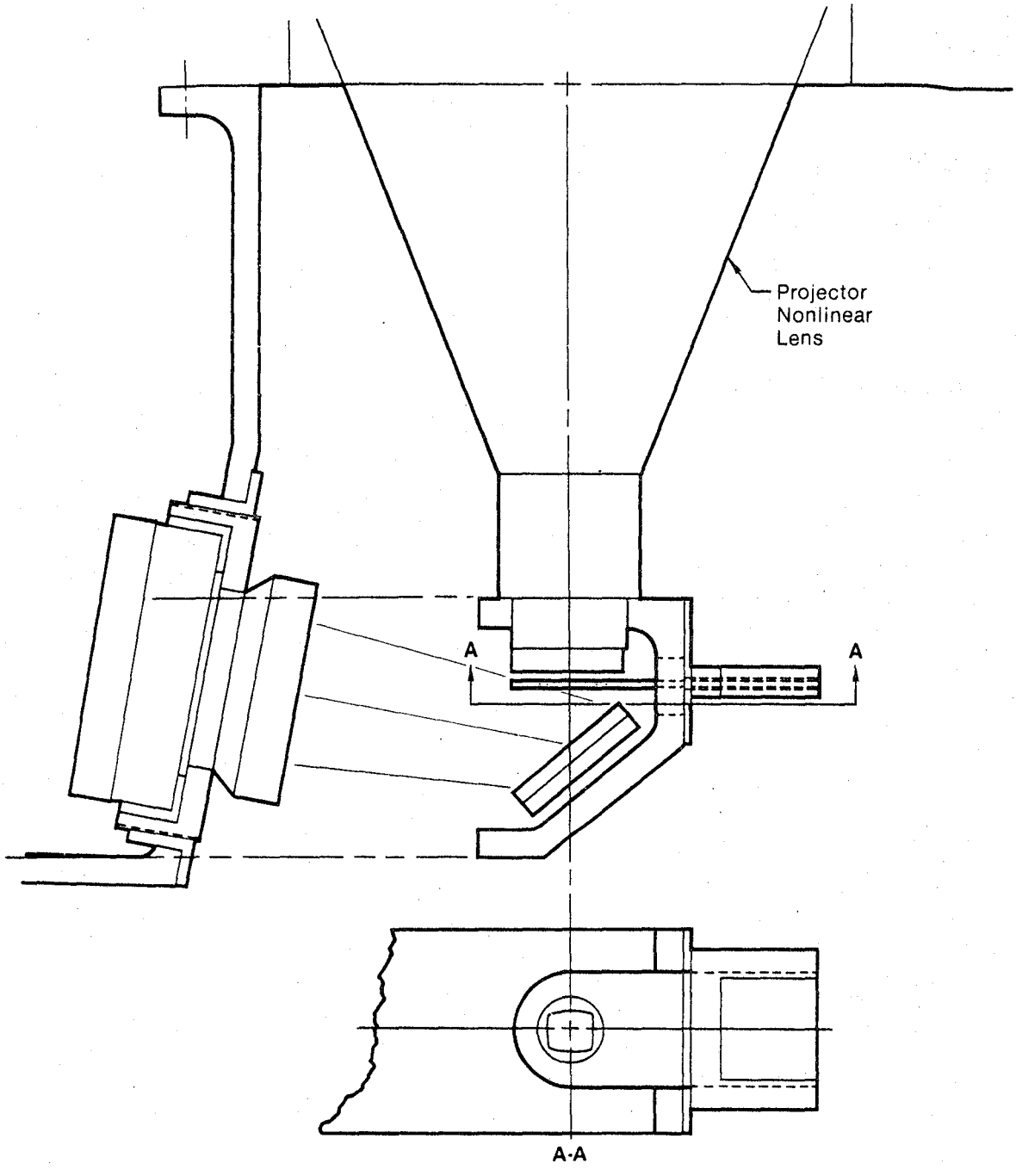

Figure C-2. Format Mask Installation

APPENDIX D

COMPUTER GENERATION OF VARVS IMAGERY (RELATED EFFORT)

The non-linear display has been adapted to flight simulation by using computer generated imagery. The entire 160° field requires no more computa-ational capability than a conventional 525 line TV display. An IRAD effort was begun about 1 year ago to determine its feasibility for computer generated images on a simulator.

The extreme non-linearity between the image and display surface dictates independent computation for every pixel in the non-linear lens focal plane. A special purpose computer is therefore reuqired in order to make the transformation between earth coordinates and non-linear lens image plane coordinates in real time. The approach is to compute sequentually with raster scan position the location on the ground plane of each pixel on the non-linear lens focal plane and determine the intensity of this point, using the digital ground data base. For the purpose of developing the approach a uniform linear grid was selected as a ground data base.

The theory involves a series of coordinate transformation matrices. The first defines the output vector on the non-linear lens (Figure D-1) as a function of focal plane coordinates x', y'. Since the basic lens equations, Table 1, are in polar form, the first conversion involves computing ρ, θ from x', y'.

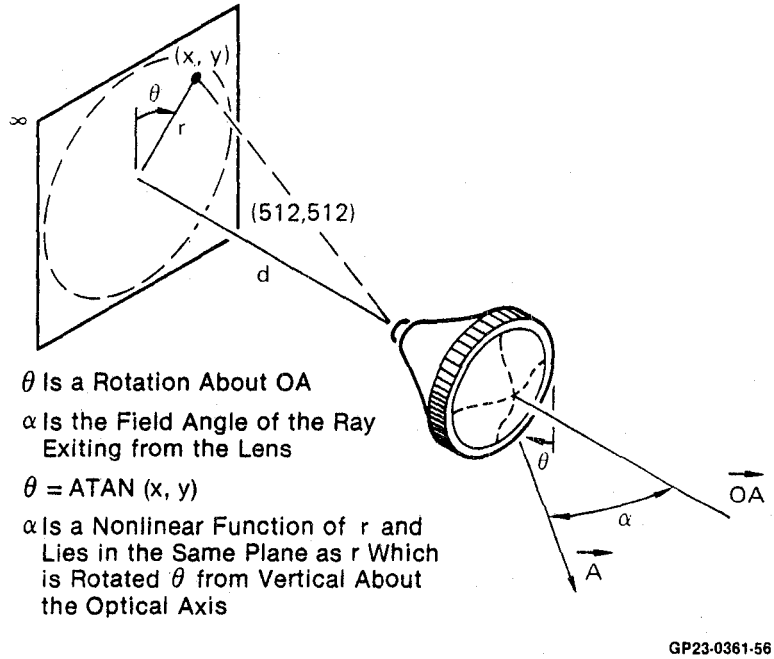

Figure D-1. Nonlinear Lens Geometry

Next, ρ is converted to α per the lens equations, Table 1. The lens output vector relative to the lens optical axis can then be defined by the matrix

$$\bar{A} = \begin{matrix} a_1 = \sin\alpha \cos\theta \\ a_2 = \cos\alpha \\ a_3 = \sin\alpha \sin\theta \end{matrix}$$

This vector must then be converted to ground coordinates β, as shown in Figure D-2. This is accomplished by a conventional coordination transformation matrix, [Q] i.e.,

$$\beta = [Q]\,\bar{A}$$

Finding the ground intersection is now simple. Vehicle altitude is divided by the vertical direction cosine to compute vector length, R, which is then multiplied by the other two direction cosines to locate the intersection point relative to the aircraft position, Δx, Δy. Aircraft position is then combined with these to establish an absolute ground point location X,Y.

These coordinates are then referenced to the data base for intensity information. In the case of the grid this can be done very simply by using a tolerance band on lower order bits.

The implementation of the non-linear lens C.G.I. equations in real time presents a difficult task. If we consider that the TV raster consists of 512 lines each with 512 elements, the lens image (consisting of a circle inscribed on a square format) will contain nominally 205K pixels, each of which must be updated 30 times a second. Thus, more than 6 million pixels must be calculated each second. A special purpose computer with pipeline architecture is needed to perform at the necessary throughput rate.

To evaluate the processing requirement in more detail a brute force method, flow-charted in Figure D-3, was implemented on a PDP 11/40 minicomputer and displayed with a Quantex DS-20 Image Processor. This allows a non-realtime evaluation of C.G.I. results.

TABLE D1. NONLINEAR LENS EQUATIONS

$\alpha = \rho/30.0$ for $0 \leqslant \rho < 0.0498$,

$\alpha = 0.001727 \cdot (\rho + 11.32)^{1.733}$ for $0.0498 \leqslant \rho < 0.5685$

and Finally

$\alpha = \left(\frac{(455.3 \cdot \rho)}{796}\right) - 2.58$ for $0.5685 \leqslant \rho \leqslant 1.0$

GP23-0361-24

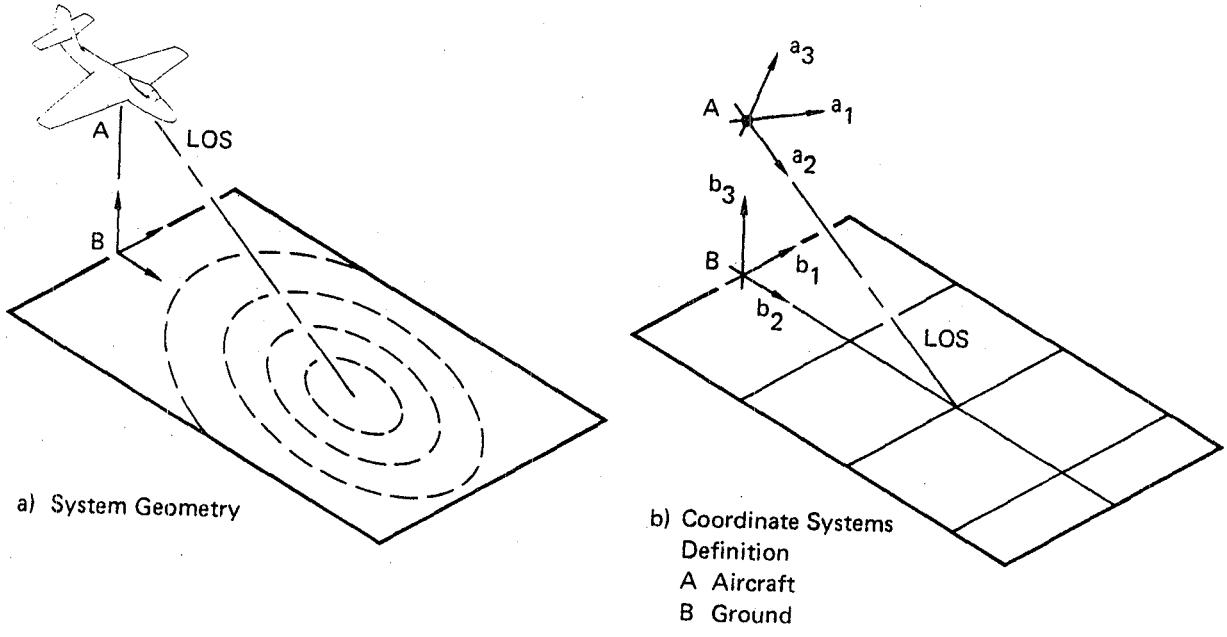

Figure D-2. Mission Geometry

GP23-0361-57

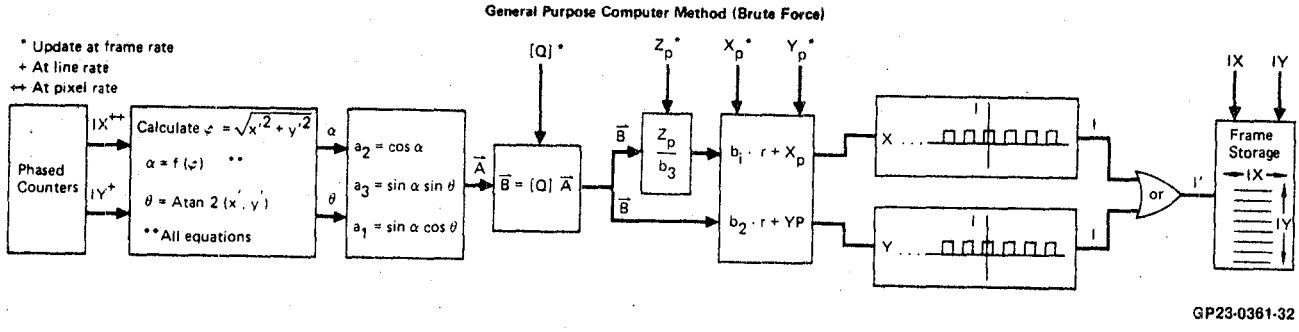

GP23-0361-32

Figure D-3. Nonlinear Lens Grid Calculation Flow Diagram

Three imagery sets were compiled: 1) single frames of the ground grid at different system viewing geometries, 2) specialized grids for projector alignment, and finally 3) sequential frames to be used to simulate real time C.G.I. Some of these are shown in Figures D-4 through D-7. They require about 50 minutes each to complete. These images were put on video tape and statically displayed at NASA. Results were good enough to justify further design.

In order to achieve an acceptable real time computer-generated image display the C.G.I. equipment must be capable of outputting nearly 6.2 million pixels per second, or one pixel every 161 nanoseconds. It is clear that only additions and multiplications can be performed in this time. This dictates the organization shown in Figure D-8. Look up tables are utilized to solve the lens equations and to establish vector length. These tables are large but certainly not prohibitive.

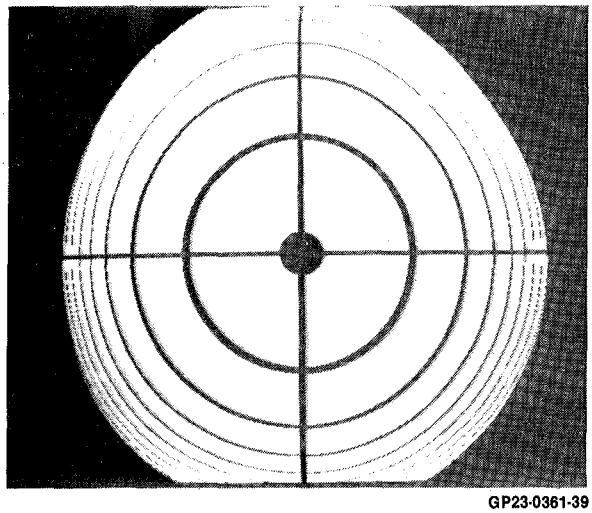

GP23-0361-39

Figure D-4. Computer Generated Alignment Image

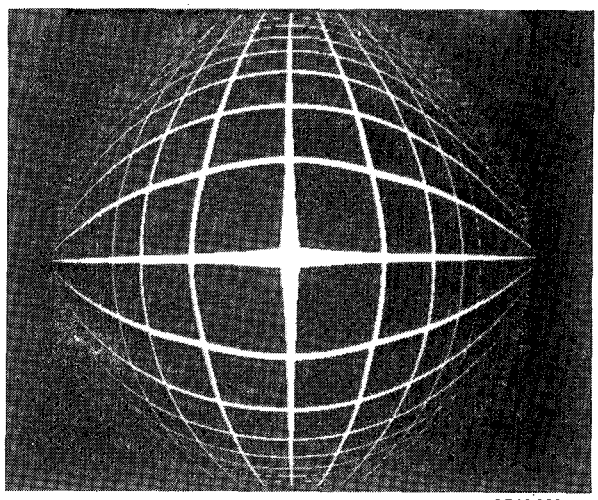

GP23-0361-40

Figure D-5. Computer Generated Image, 90° Depression Angle

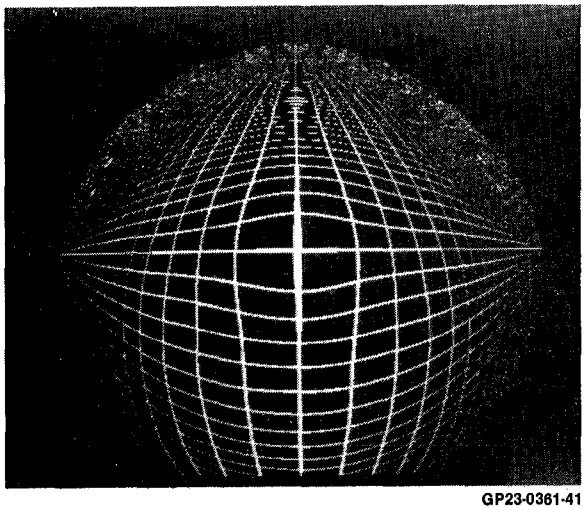

GP23-0361-41

Figure D-6 Computer Generated Image, 30° Depression Angle

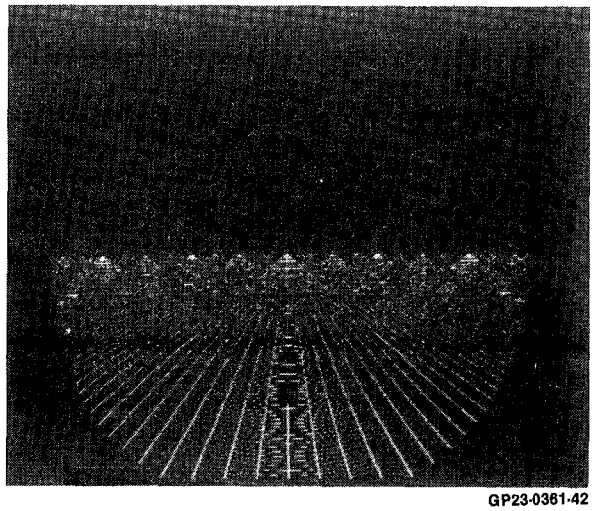

GP23-0361-42

Figure D-7. Computer Generated Image, 0° Depression Angle

The approach was simulated on a HP 1000 computer to evaluate logic, word length, memory size, etc. In general, only minor refinements were required and hardware design was initiated. We hope to have this completed so that demonstrations can be made at NASA by late 1982.

D.1 CONCLUSION

A Variable Acuity Display appears feasible and may be useful in many simulator applications. The result could be equipment simplifications since a single TV channel could generate the entire visual field as compared to 3 or more TV channels required for current systems.

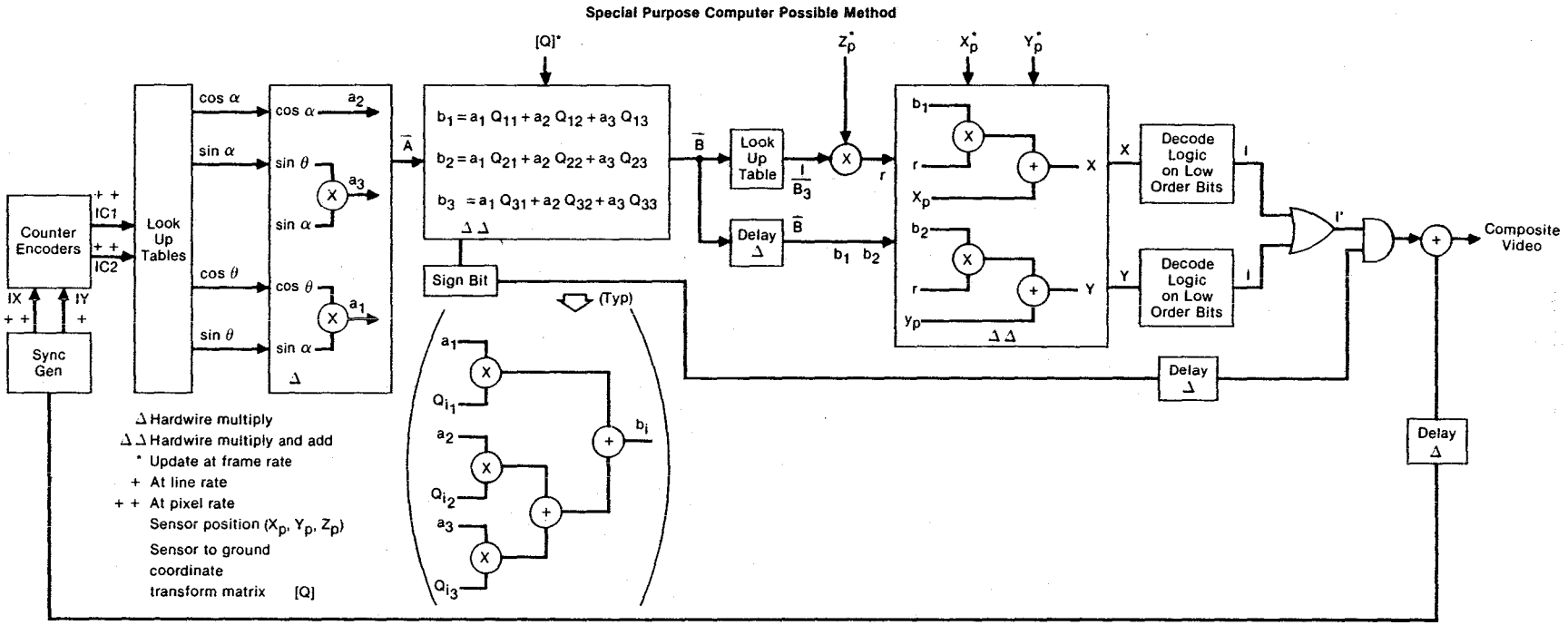

Figure D-8. Nonlinear Lens Grid Calculation Flow Diagram

GP23-0304-9

This Page Intentionally Left Blank

References

1. Helmic, R.D. et al, A Non-Linear Lens For Bandwidth Reduction in Military TV System Applications, Final Report, Contract N00014-73-C-0154, Office of Naval Research, Department of the Navy, Arlington, VA., Nov. 1973

2. Fisher, R.W., Remote Viewing System, Final Report, ONR-CR-213-129-2F, Contract N00014-75-C-0660, Office of Naval Research, Department of the Navy, Arlington, Va., May 1977.

1. Report No.	2. Government Accession No.	3. Recipient's Catalog No.
NASA CR-170404		

4. Title and Subtitle	5. Report Date
VARIABLE ACUITY REMOTE VIEWING SYSTEM FLIGHT DEMONSTRATION	July 1983
	6. Performing Organization Code

7. Author(s)	8. Performing Organization Report No.
Ralph W. Fisher	MDC IR0296
	10. Work Unit No.

9. Performing Organization Name and Address	11. Contract or Grant No.
McDonnell Aircraft Company Box 516 Saint Louis, Missouri 63166	NAS4-2619
	13. Type of Report and Period Covered

12. Sponsoring Agency Name and Address	13. Type of Report and Period Covered
	Contractor Report — Final
National Aeronautics and Space Administration Washington, D.C. 20546	14. Sponsoring Agency Code
	RTOP 199-53-05-01

15. Supplementary Notes

NASA Technical Monitor: Terrence W. Rezek, NASA Ames Research Center, Dryden Flight Research Facility, Edwards, CA 93523.

16. Abstract

The Variable Acuity Remote Viewing System (VARVS), originally developed under contract to the Navy (ONR) as a laboratory brassboard, was modified for flight demonstration. The VARVS system was originally conceived as a technique which could circumvent the acuity/field of view/bandwidth tradeoffs that exists in remote viewing to provide a nearly eye limited display in both field of view (160°) and resolution (2 min arc) while utilizing conventional TV sensing, transmission, and display equipment. The modifications for flight demonstration consisted of modifying the sensor so it could be installed and flown in a Piper PA20 aircraft, equipped for remote control and modifying the display equipment so it could be integrated with the NASA Research RPB (RPRV) remote control cockpit.

17. Key Words (Suggested by Author(s))	18. Distribution Statement
Variable acuity, Optics, Vision, Displays, Remote sensing, Television system, Optical detection, Flight simulation	Unclassified-Unlimited STAR category 06

19. Security Classif. (of this report)	20. Security Classif. (of this page)	21. No. of Pages	22. Price*
Unclassified	Unclassified	68	A04

*For sale by the National Technical Information Service, Springfield, Virginia 22161.

End of Document